Contrasting the effects of nitrogen form and concentration on primary producer biomass, cyanotoxins, and microbiome structure in eutrophic and mesotrophic lake communities

By
© 2021
Janaye Hanschu
B.S., Kansas State University, 2017

Submitted to the graduate degree program in Ecology and Evolutionary Biology and the Graduate Faculty of the University of Kansas in partial fulfillment of the requirements for the degree of Master of Arts.

Chair: Amy J. Burgin

Benjamin Sikes

Lydia Zeglin

Date Defended: 22 July 2021

The thesis committee for Janaye Hanschu certifies that this is the approved version of the following thesis:

Contrasting the effects of nitrogen form and concentration on primary producer biomass, cyanotoxins, and microbiome structure in eutrophic and mesotrophic lake communities

Chair: Amy J. Burgin

Date Approved: 29 July 2021

Abstract

Cyanobacterial harmful algal blooms (cyanoHABs) are becoming more frequent and intense due to anthropogenic activities. CyanoHABs degrade water quality and impose threats to human and ecosystem health. Yet, we do not fully understand under which circumstances a bloom turns toxic. Recent research has shown that although increased phosphorus (P) stimulates algal biomass and shifts the community over to cyanobacteria, excessive nitrogen (N) may be responsible for the toxicity of a cyanoHAB. A cyanotoxin contains seven amino acids creating a N-rich molecule, and therefore, requires N. In this study, we asked: (1) What form of nitrogen fuels toxic cyanoHABs? (2) How does prior bloom history from a lake affect the propensity to stimulate blooms with added nitrogen? We used replicate 300 L aquatic mesocosms filled with lake water from a mesotrophic (low nutrient) lake and a eutrophic (high nutrient) lake, to which we added different N additions. We show the microbiome of the lake is the most responsible for determining a potential cyanoHAB. Furthermore, the eutrophic lake responded more strongly to additions of nitrogen compared to the mesotrophic lake. Cyanobacteria became more abundant in the ammonium mesocosms in the eutrophic lake relative to the other bacteria present, while chloroplasts become more abundant in the nitrate mesocosms indicating nitrate stimulate a green or yellow green bloom instead of a cyanoHAB. Despite the presence of cyanobacteria, toxin (microcystin-LR) concentrations were below detection limit in the water column and low in the sedimented microbe samples. The lack of toxin could be due to the methodology behind quantifying toxins, a lack of trigger for producing toxins by the cyanobacteria that were present, or an absence of toxin-producing bacteria from the microbial community. Management strategies should be aimed at alleviating eutrophication in lakes by managing for excess N.

Acknowledgments

First, I would like to thank my mentor, Dr. Amy Burgin, for her patience, understanding, and wisdom. She supported me through all obstacles in my academic and personal life. She recognized my fears I was scared to admit and helped extinguish them by offering guidance.

I would also like to thank my committee members, Dr. Lydia Zeglin (Kansas State University) and Dr. Ben Sikes. I worked with Dr. Zeglin as an undergrad and then as a research assistant. She helped cultivate my interests and recognized my enthusiasm for aquatic systems and water quality. Dr. Sikes challenged me to look at problems in new light and pushed me to expand the scope of my research.

Many thanks to Bri Richards, lab manager, who is consistently organized and ready to find a solution. Thank you to Samantha Thomas, data manager for EPSCoR MAPS project, who helped me understand computers and their power.

Thanks to Abagael Pruitt, who was the undergraduate who worked on the experiment with me, for the many laughs and the get-it-done attitude.

Thanks to all the Burgin-Loecke lab members for their hard work and dedication.

Thank you to the University of Kansas Field Station (KUFS) staff, Bruce Johanning, Vaughn Salisbury, and Sheena Parsons for helping with the logics of moving gallons of lake water, setting up the mesocosms, and helping to overcome any logistic problem.

I would like to thank Michelle Kelly, former KU master's student, for the courage to go to graduate school and for all the support along the way.

Thanks to Alex Wohler who ran microbial samples when I could not due to pregnancy and the pandemic.

And thank you to my family, who has supported and encouraged me unconditionally through the pandemic, pregnancy complications, and motherhood while being a graduate student.

Table of Contents

Abstract iii

Acknowledgments iv

List of Figures vii

List of Tables viii

Chapter 1: Lake Microbiomes Differ in Response to Nitrogen Additions 1

Introduction 1

Methods 4

Experimental Design 4

Water and Sediment Sample Collection 8

Analytical Chemistry Methods 10

Microbiome Molecular Methods 11

Data Analysis and Statistical Methods 12

Results 13

Discussion 25

Conclusion 30

References 31

Supplemental Information 44

List of Figures

Figure 1: *Conceptual model* 1

Figure 2: Mescosom schematic 5

Figure 3: *Chl-a concentration and dissolved oxygen in the water column* 14

Figure 4: *Chl-a concentrations in the sedimentation* 15

Figure 5: *Microcystin concentrations in the sedimentation* 16

Figure 6: *PCoA of water column microbial community composition (MCC)* 17

Figure 7: *Water column genus level microbial taxonomic abundance and composition* 19

Figure 8: *Water column Microcystis genus abudnance and composition* 20

Figure 9: *PCoA of sediment microbial community composition (MCC)* 22

Figure 10: *Sedimentation genus level microbial taxonomic abundance and composition* 23

Figure 11: *Sedimentation Microcystis genus abudance and composition* 24

List of Tables

Table 1: *Contrasting the histories of each lake type*..... 6

Table 2: *Water column and sediment PERMANOVA results* 18

Chapter 1: Lake Microbiomes Differ in Response to Nitrogen Additions

Introduction

Primary producers drive biogeochemical cycling in aquatic systems through nitrogen fixation, denitrification, supplying dissolved oxygen and up taking carbon dioxide, a potent greenhouse gas, by photosynthesis (Paerl et al. 2018). However, under increased nutrient loading, primary producers can grow unabated creating high amounts of biomass from the excess nutrients (i.e., eutrophication) (Qin et al. 2020; Paerl et al. 2020). Human activities such as agricultural development have increased the frequency and intensity of eutrophication through both point and nonpoint sources of nutrient loading (Paerl et al. 2001; Carmichael et al. 2001; Paerl and Barnard 2020). Eutrophication can result in Cyanobacteria harmful algal blooms (cyanoHABs) that threaten water quality, which can have major ramifications for both human and ecosystem health (Brooks et al. 2016; Carmichael and Boyer 2016). Cyanobacteria produce cyanotoxins that harm other organisms and humans including neurological, kidney, liver, skin, and digestive issues (Carmichael et al. 2001; Testai et al. 2016; Svirčev et al. 2017; Bouaïcha et al. 2019; Chorus and Bartram 2021). Reduced water quality can lead to economic burdens including recreation, property values, and drinking water (Chorus et al. 2000; Dodds et al. 2009). Therefore, understanding the linkages between the development of cyanoHABs, nutrient inputs, and cyanotoxin production is critical for global health (Wilhelm et al. 2020; Massey et al. 2020; Figure 1).

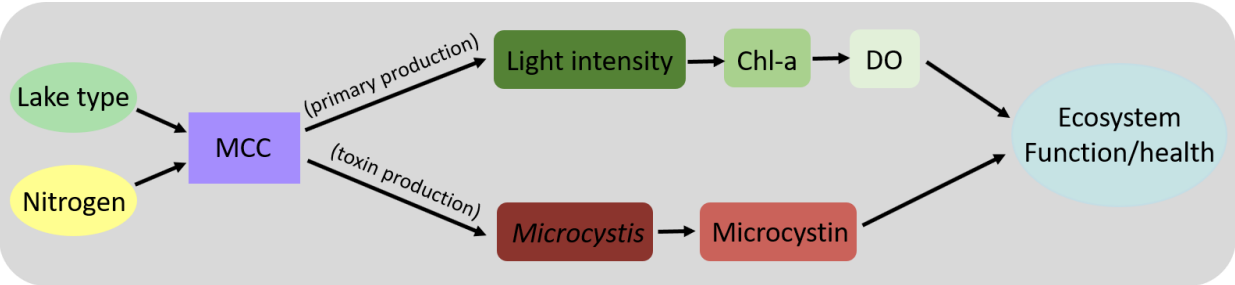

Figure 1: *Conceptual model depicting the influence of lake type and nitrogen on the microbial community composition (MCC), and therefore, ecosystem function/health.*

Many Cyanobacterial species are capable of nitrogen fixation allowing the species to sustain high growth rates in N limited waters (Paerl and Otten 2016). N has been found to be tightly correlated to higher abundance of toxic species/strains (Davis et al. 2010, Monochamp et al., 2014) or to an increase in cyanotoxin concentrations when toxic species/strains are present (van de Waal et al., 2014). CyanoHABs have been found to dramatically increase when epilimnion nitrogen to phosphorus (N:P) ratios fall below 29:1 by weight, and become rare when N:P exceeds this ratio (Smith 1983b). The phylum of Cyanobacteria is diverse, and not all species can fix N. Non-N fixing species become rich in the presence of N-fixing species when N is finite. However, N-fixation is a metabolically expensive biogeochemical process, and as bioavailable forms of N such as nitrate and ammonium become more prevalent, Cyanobacterial communities could become more dominant, specifically toxin producing Cyanobacteria (Donald et al. 2011; Chaffin et al. 2018). N form appears more important in eutrophic waters where overall nutrients are already high, including P (Smith 1983b). Therefore, N form appears to be significant when producing a toxic bloom, especially under different environmental conditions.

The chemical structure of cyanotoxins fall into three groups: cyclic peptides, alkaloids and lipopolysaccharides (LPS). The most common are cyclic peptides that contain seven amino acids (Sivonen and Jones 1999). Due to these N-rich chemical structures, cyanotoxin production requires abundant nitrogen (Wagner et al. 2021). The different combinations create more than 200 variants, which can vary in toxicity (Metcalf and Souza 2019; Chorus and Welker 2021). Despite N being required for toxin production, we do not understand the environmental factors that favor cyanotoxin production. (Berry et al. 2017). The phylum of Cyanobacteria is diverse. In parallel to all species not being able to fix N, not all species produce toxins. A bloom can be toxic or non-toxic presumably depending on extracellular environmental conditions. Blooms are

photoautotrophic, and therefore, generally favor conditions with ample light for photosynthesis, shallow water to maximize exposure to light, little mixing of the water column with calm winds, warmer temperatures, and N and phosphorus (P) enriched waters (Smith 1986; Paerl et al. 2001; Zanchett and Oliveira-Filho 2013). Although phosphorus contributes to eutrophication in lakes (Carpenter et al. 1998; Smith 2003), toxin production also depends on N. As global N increases, Cyanobacteria communities can shift and cause rampant toxic cyanoHABs. (Paerl and Otten 2016b; Gobler et al. 2016; Levy Sharon 2017). However, this community shift is poorly understood (Berry et al. 2017). Consequently, it is important to understand which environmental conditions may cause a bloom to become toxic.

Microcystins (MCs) are the most frequently occurring cyanotoxin (Zurawell et al. 2005). MCs are released by certain species within the genera *Microcystis*, *Anabaena*, *Planktothrix*, and *Nostoc* (fresh- and saltwater). MCs are monocyclic heptapeptides that contain seven amino acids. There are over 200 MC variants (Spoof and Catherine 2016), and the derivative variant, microcystin-leucine arginine (MC-LR) is the most abundant and toxic cyanotoxin and is known to be produced by certain *Microcystis* spp. (Zurawell et al. 2005; Linville et al. 2009). MC-LR accounts for 46-99.8% of the total MC concentrations in blooms (Vasconcelos et al. 1996). MC-LR is mutagenic, carcinogenic, and lethal to humans and animals (Imanishi and Harada 2004). In our experiment, we focused efforts to measured microcystin-LR (MC-LR) and not all cyanotoxins.

We used aquatic mesocosms and a two-factor repeated-measures design to examine the effects of N form (nitrate vs. ammonium) and concentration (high vs. low) on lake microbiome structure, toxin production, and ecosystem properties between two lakes (mesotrophic vs. eutrophic). This study investigated two main questions: (1) What forms and concentrations of nitrogen fuels toxic cyanoHABs? (2) How does prior bloom history from a lake affect the

propensity to stimulate blooms with added nitrogen? We hypothesized that N form drives toxicity (Question 1). N inputs into lakes are largely in the form of NO_3^- and secondarily NH_4^+ (Donald et al. 2011). NO_3^- is often at far higher concentrations because the most biologically available N form is NH_4^+. NH_4^+ diffuses across cellular membranes and then can be promptly integrated into amino acids and proteins (Herrero et al. 2001; Finlay et al. 2010). In contrast, NO_3^- is more energetically expensive because NO_3^- actively transports across the cellular membrane, which requires adenosine triphosphate (ATP). Thereafter, NO_3^- is reduced to nitrite and then reduced further to NH_4^+ (Flores et al. 2005). Because NH_4^+ is more biologically available, NH_4^+ is used at a faster rate than NO_3^-, leaving NO_3^- as the highest concentration N source for aquatic microorganisms. We also hypothesized that the eutrophic lake will respond to N additions and have a higher potential to produce a toxic cyanoHAB than the mesotrophic lake type (Question 2) because lakes that are accustomed to higher nutrient loads already contain more Cyanobacteria (Wilhelm et al. 2011)

Methods

Experimental Design

We filled a total of 30 ~300 L mesocosms in a greenhouse with water from a mesotrophic lake (n = 15) and a eutrophic lake with a known history of previous cyanoHABs (n = 15; Figure 2). For each lake type, five different N treatments were added in triplicate. Treatments included a control (no nutrient addition), high ammonium (1 mg/L NH_4^+-N), high nitrate (20 mg/L NO_3^--N), low ammonium (0.5 mg/L NH_4^+-N), and low nitrate (2 mg/L NO_3^--N). The experiment ran for three weeks from July 30th to August 19th of 2019. Initial N additions were added after day 1 (July 30th) sample collection. hold N concentrations at the target level, we added NH_4^+ each week and NO_3^- as needed. NH_4^+ was resupplied more regularly because it is the more bioavailable form of

N. Concentrations were monitored by daily nitrate and ammonium sampling and analyzing (Supplemental Info Figure B).

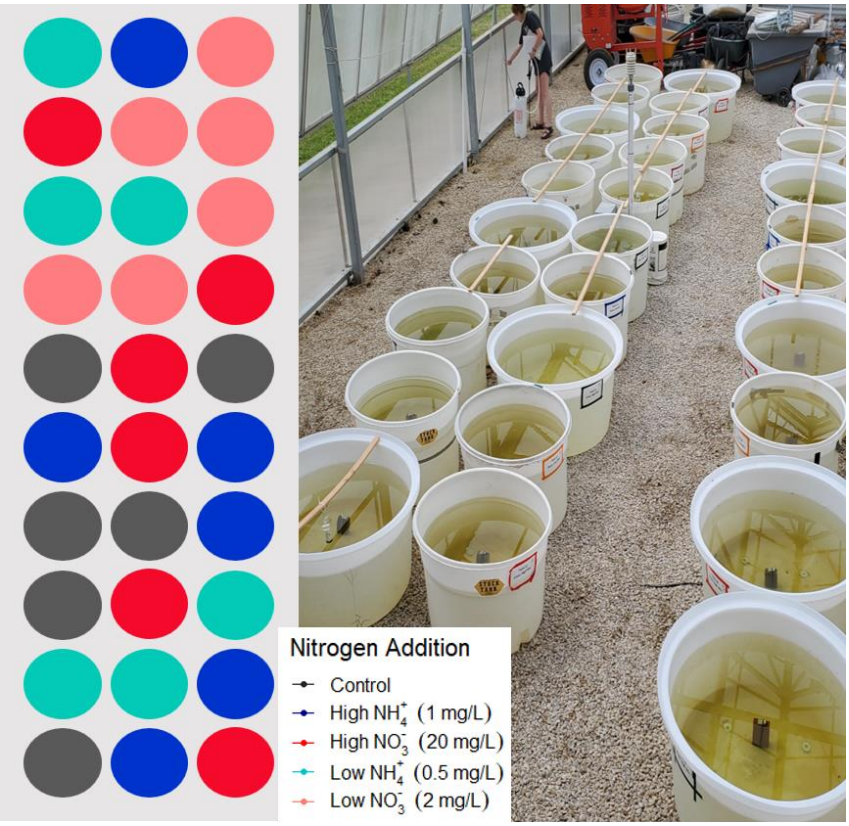

Figure 2: *Mesocosm schematic. To reduce potential bias, mesocosms were randomly assigned to lake type/N addition. Within the lake type, mesocosms were inoculated with different N forms (NH_4^+ vs. NO_3^-) and concentrations (high vs. low) in triplicate.*

The lake water used for the experiment originated from two lakes in Northeast Kansas (Table 1). The mesotrophic water was from Cross Reservoir (39.0518˚N, 95.1846˚W), which is a small impoundment—3-ha surface area, 12 m maximum depth with protected watershed of 50-ha dominated by grasslands and forests (53% grassland and 42% forest), created in 1991. The lake has no records of cyanoHABs and had nutrient concentrations of 6.3 µg/L NH_4^+-N and 0.45 mg/L SRP-P before we filled the mesocosms (*n=1*). In contrast, the eutrophic water from Perry Reservoir (39.2265˚N, 95.4442˚W) is historically prone to periodic cyanoHABs and had nutrient concentrations of 8.6 µg/L NH_4^+-N and 0.35 mg/L SRP-P before we filled the mesocosms (*n=1*). Perry Reservoir is a larger impoundment—4046-ha surface area, 13 m maximum depth with a 280,802-ha watershed comprising cropland and grassland (33% cropland and 52% grassland),

created in 1964. These two lakes with contrasting histories were used to assess if baseline nutrient levels and microbial communities shift toward a cyanoHAB under added N pressures.

Contrasting lake histories: mesotrophic vs. eutrophic		
	Cross Reservoir (mesotrophic)	**Perry Reservoir (eutrophic)**
Surface area	3 ha	4046 ha
Maximum depth	12 m	13 m
Year constructed		1964
Watershed size	50 ha	280,802 ha
% Grassland	53 %	52 %
% Cropland		33 %
% Forest	42 %	
NH_4^+-N	0.0063 mg L^{-1}	0.0086 mg L^{-1}
NO_3^--N	Below detection limit	Below detection limit
SRP-P	0.8021 mg L^{-1}	0.4278 mg L^{-1}

Table 1: *Contrasting the histories of each lake type: mesotrophic vs. eutrophic. Cross reservoir data is from Chapin et al. 2004. Perry Reservoir data from the U.S. Army Corps of Engineers.*

While P is a well-established control on lake eutrophication (Hutchinson 1972; Schindler 1975; Smith 1983b; Paerl and Otten 2013), however, recent studies have shown cyanoHAB development and toxin production become more intense when there is more N (Finlay et al. 2010; Donald et al. 2011; Monchamp et al. 2014). However, other studies have found that Cyanobacteria have a diverse and varied response to N vs. P enrichment (Dolman et al. 2012). Therefore, in preparation for the larger experiment, we conducted a pilot study. The pilot study used lake water from the mesotrophic lake (Cross Reservoir). Both N and P treatments were added in triplicate to 18 mesocosms for 12 days in March 2019. Elevated Chl-a concentrations were only found in the N addition mesocosms. Chl-a in the P addition mesocosms did not significantly differ from the controls (Supplemental Info Figure A). Therefore, we did not impose a P addition treatment in the full experimental design.

N addition treatment decisions were rooted in the literature, biological processes that uptake N, and local environmental conditions. The high N concentrations reflect concentrations

found in agricultural regions whereas the low concentrations reflect chemistry found in grassland regions. The specific magnitude of concentrations was based on two ongoing projects that are components of the NSF-ESPCoR Kansas MAPS project. In the first project, data from agriculture streams and grassland streams dominated subwatersheds within the larger Delaware River basin, which drains to our eutrophic lake (Perry Lake). Agricultural streams consistently had higher nitrate and ammonium concentrations than grassland streams (19.3 NO3-N mg/L vs. 0.97 NO3-N mg/L; Kynser Wahwahsuck Master's thesis personal communication); thus concentrations for the nutrient additions were selected to reflect the water draining these different land use. In the second project, data was gathered on leachate from soil mesocosms collected from agriculture and grasslands across Kansas.

Before the experiment, the mesocosms were power washed to physically remove potential contaminants. They were then soaked with bleach for 10 minutes to degrade residual DNA and rinsed three times with distilled water to wash away the bleach. Mesocosms were then filled with mesotrophic and eutrophic lake water. Before initial N additions, we sampled and analyzed NH_4^+, NO_3^-, and soluble reactive phosphorus (SRP) (Supplemental Info Figure B). We did a full suite of sampling in the morning of July 30th 2019, referred to as sample day 1. We then added N and sampled again for NH_4^+, NO_3^-, and SRP to ensure we hit our target concentrations in each mesocosm. We continued to sample for NH_4^+, NO_3^-, and SRP daily to confirm mesocosms were receiving an N treatment. Additionally, we collected water column samples and sediment samples. The sediment samples are an accumulation of the water column samples as organic matter from the water column settles to the bottom of the mesocosm. These two different sample types could vary over time. We also deployed sensors that monitored dissolved oxygen and light intensity.

Samples were analyzed for chlorophyll-a (chl-a), a cyanotoxin, and eDNA. Sediment samples were also collected for total suspended solids (TSS) and ash-free dry mass (AFDM).

Water and Sediment Sample Collection

Water column samples were collected every day for the first 10 days of the experiment (sample days 1-10) and then collected every other day during the remaining duration of the experiment (sample days 10-14). All water column samples were collected from the middle of the mesocosm in the top 15 cm. In the lab, all bottles, syringes, and other sampling materials were rinsed three times with hot tap water, three times with RO water, and three times with 18MΩ water. Materials used for eDNA sampling were sterilized in the autoclave. In the field to collect the water column samples, we first rinsed all supplies with the appropriate mesocosm water three times. Rinse water was discarded outside of the mesocosm. To ensure a treatment affect, we monitored NH_4^+, NO_3^-, and SRP by field filtering whole mesocosm water through a disposable 0.45 µm syringe filter into a triple rinsed HDPE bottle. To understand how N additions affected biomass growth, we took chl-a measurements from the water column. Mesocosm water was field filtered through a 1 µm Glass Fiber type A/E Pall filter. The water was discarded, and the filter was reserved for chl-a analysis. Upon collection, the chl-a filter was kept out of the light and placed on ice until transported back to the lab and stored at -20˚C until processing. To understand if N additions increased cyanotoxin concentrations, mesocosm water was collected in amber brown glass bottles to prevent light degrating, placed on ice for transportation, and stored at -20 ˚C until processing. The filtered samples were then stored at 4˚C and analyzed within a week's time. To sample for the microbiome community, we used sterile technique to filter 60 mL of water through a 0.22 µm hydrophilic polyethersulfone filter. The filters were reserved for environmental (eDNA). The filters were placed in 2.0 mL cryovials and immediately dropped into liquid N and

stored at -80˚C. A multiparameter water quality meter (YSI ProDSS) analyzed dissolved oxygen (DO) of each mesocosm.

Sedimentation happens when suspended solids settle out of the water column into the benthic zone. In some frameworks, sediment is composed mainly of minerals and other inorganic or organic matter. In the context of this experiment, sediment refers to organic matter that has settled out of the water column to the bottom of the mesocosm. Four sediment traps (weighted petri dishes) were deployed on sample day 2 (July 31st 2019). On sample day 9 (Aug. 30th 2019), two traps were collected. The remaining two traps were collected on sample day 14 (Aug. 19th 2019). One trap was used for total suspended solids (TSS) and ash free dry mass (AFDM) while the other trap was allocated equally for chl-a, cyanotoxin, eDNA analysis, and for an archived sample. Sediment samples were put on ice for transport back to the lab and stored at -20˚C. Because the sediment samples were stored at -20˚C instead of -80˚C, we did a small experiment to compare the two storage temperatures. We collected eight of the same samples from a nearby pond. Four of the samples were stored at -20˚C and four were stored at -80˚C. All eight samples were sequenced together. The storage temperature resulted in different microbial communities (Supplemental Info Figure C).

We collected light intensity from each mesocosm to see if shading affected the algal response. HOBO pendant data loggers placed in the middle of each mesocosm logged relative light intensity every 5 minutes. Light intensity was averaged between 8 am and noon for each mesocosm because all other sample collections took place between 8 am to noon. We then compared this data to photosynthetically active radiation (PAR) data collected from outside the greenhouse. PAR data was provided by the National Ecological Observatory Network (NEON) station (39.04043, -

95.19215) 645 m away from the greenhouse (39.047667, -95.193649). Light data in all replicate mesocosms followed the same trends (Supplemental Info Figure D).

Analytical Chemistry Methods

Dissolved NH_4^+-N was determined on filtered water column samples following protocols from Kérouel and Aminot 1997. Samples were analyzed on a Shimadzu UV-1280 UV-VIS Spectrophotometer. Dissolved NO_3^--N measurements were measured using a Dionex ICS-900 Ion Chromatograph (Dionex, Sunnyvale, California). SRP-P was measured on a Smartchem 200 discrete analyzer using the method 410-200B (2011) from Westco Scientific Instruments, Inc. Samples for Chl-a and cyanotoxins from the water column and sediment were quantified using the same methods. Chl-a was quantified using a 10-AU Fluorometer. All samples were calibrated to a nine-point standard curve with blank checks every 12 samples. Water column samples were normalized to the volume pushed through the filter (60 mL) and sediment samples were normalized to the area of the divided trap (0.006 m^2).

MC-LR was quantified using the enzyme-linked immunosorbent assays (ELISA) with the microcystins-ADDA kit (Abraxis, Warminster, PA) following the manufacturer's protocol. MC samples were lysed using freeze/thaw cycles. The instruments that analyzed the samples were calibrated to a six- to eight-point standard curve. Blanks and drift checks were measured every 10 samples.

Sediment total suspended solids (TSS) and ash free dry mass (AFDM) were determined by collecting the contents captured in sediment traps that were then pulled through pre-ashed 1 µm glass fiber type A/E Pall filters with a vacuum. Filters were dried in a desiccator for >24 hours. The net weight was calculated and standardized to the area of the trap to find TSS (TSS_mg/m^2 = (DryFilterWt_g - InitialFilterWt_G) *0.02434 m^2). The same filters used for TSS were then placed

in a preheated (530˚C) muffle furnace for 15 minutes. Filters were removed and were allowed to cool for 1 minutes, then placed back into the furnace for another 15 minutes. The net weight of the dried filter and the ashed filter was standardized to the area of the trap to find AFDM (AFDM_mg/m^2=(DryFilterWt_g - AshedFilterWt_g)*0.02434 m^2). All chemistry analyses were done at the University of Kansas.

Microbiome Molecular Methods

To examine microbiome community structure, samples were extracted for total genomic gDNA from the water column and sediment. Half the filter that was used to catch water column biomass (approximately 30 mL water), and approximately 0.5 g of homogenized sediment were extracted. The sample was physically lysed using lysis beads, in a solution of 0.5 mL cetyltrimethylammonium Bromide (CTAB), 50 uL of 0.1 M (NH4)Al(SO4)2, and 0.5 mL phenol:chloroform:isoamyl (25:24:1). Overnight precipitation in PEG 6000 was used to extract the RNA and eDNA (DeAngelis et al. 2010). The gDNA yields were quantified using a Quant-it PicoGreen assay kit (Life Technologies, Grand Island, NY). The gDNA was standardized per milliliter gram of water sample or sediment, respectively.

The 16S rRNA gene, region V4, was targeted for Illumina bacterial sequencing with universal bacterial primers (515F/806R) using Earth MicroBiome protocols (Caporaso et al. 2012) with two anomalies. The final concentration of the 0.04% Bovine Serum Albumin (BSA) was included with each reaction, and PCR was run for 25 cycles rather than the 35 cycles. Each DNA and cDNA sample was ran in technical triplicates for PCR. Each triplicate reaction was confirmed for amplification using gel electrophoresis. The triplicates were then pooled together for each sample. The 16S rRNA gene yield was estimated using a Quant-it PicoGreen assay kit. Amplicon amounts were normalized and combined into two separate libraries; sediment samples in one

library and water samples in another library six months later. Libraries were cleaned using a QIAquick Gel Extraction Kit and sequenced with a 2 x 150 paired-end read Ilumina MiSeq run.

Raw Illumina sequence data were processed using the QIIME2 software package v. 2020.2. Sequences were demultiplexed; due to low sequence qualities in the reverse read, only the forward reads were retained for full analysis. Quality filtering and denoising was done using the dada2 package (Callahan et al. 2016) with default parameters, and taxa were defined at the Exact Sequence Variants (ESV) level. Taxonomic assignments were made for each ESV using Bayesian Hierarchical Classifier (Gopal et al. 2012) and the SILVA database (Quast et al. 2013). Tables of ESV frequency per sample and taxonomy annotations were exported from Qiime2 for statistical analysis.

Data Analysis and Statistical Methods

Relationships between lake type and N additions in the analytical response data in the water column and sediment were examined using repeated measures analysis of variance (RM ANOVAs) and 2-way ANOVAs, respectively. Before analysis, data were log-transformed when necessary to conform to the assumption of normality and homoscedasticity within the model. For water column data, light intensity was found to be autocorrelated with DO and chl-a across the experiment's timeline (Supplemental Info Figure E). The manifestation of autocorrelation between light intensity, DO, and chl-a allowed light intensity from the NEON PAR sensor to be the covariate in the RM ANOVA models. Estimated marginal means from the RM ANOVA were used for Tukey's post hoc contrasts ($p<0.05$) to determine if the lake type differed (controls-no N addition), and which N additions differed within each lake. The sediment was only sampled twice during the duration of the experiment. Therefore, the interaction of lake and N addition were used as fixed factors in 2-way ANOVA models for the sediment data.

To examine the beta-diversity of the microbial communities within each treatment, PCoA was conducted on the 16S rDNA dataset using Bray-Curtis distances between. Permutational multivariate analysis of variances (PERMANOVA) using distance matrices and the Adonis function in the vegan package (Oksanen et al. 2020) tested pairwise dissimilarity of the community composition. The water column and the sediment had one PERMANOVA each that included sample day as a factor. To assess the relative abundance with each lake and N addition, stacked bar graphs were made using the phyloseq package (McMurdie and Holmes 2013). All data plotting and analysis was performed in the R software, version 4.1.0 (R core team, 2018).

Results

The eutrophic lake stimulated far more photosynthetic growth than the mesotrophic lake (contrasting control eutrophic vs. mesotrophic; Tukey's post hoc test, $p = 0.0023$, Figure 3a). In the mesotrophic lake, only the low NO_3^- treatment generated a response in chl-a compared to the control treatment ($p = 0.046$; Figure 3a). In contrast, the eutrophic lake type responded to all N additions ($p < 0.05$; Figure 3a) except the low NH_4^+ addition ($p = 0.7380$; Figure 3a). Analogous to the chl-a response, the eutrophic lake type produced more dissolved oxygen (DO) compared to the mesotrophic lake (controls Tukey's post hoc test, $p = 0.0001$, Figure 3b). NO_3^- treatments stimulated the most chl-a and greater DO concentrations (Figure 3). In the eutrophic lake, adding N at any concentration and either form increased the DO compared to the control mesocosms ($p < 0.05$; Figure 3b). In contrast, only the low NH_4^+ ($p = 0.0037$) and low NO_3^- ($p = 0.008$) significantly increased DO levels in the mesotrophic lake when compared to the control mesocosms. However, in the averaged mesotrophic controls, the higher DO is driven to a large outlier on sample day 11 (Supplemental Figure E).

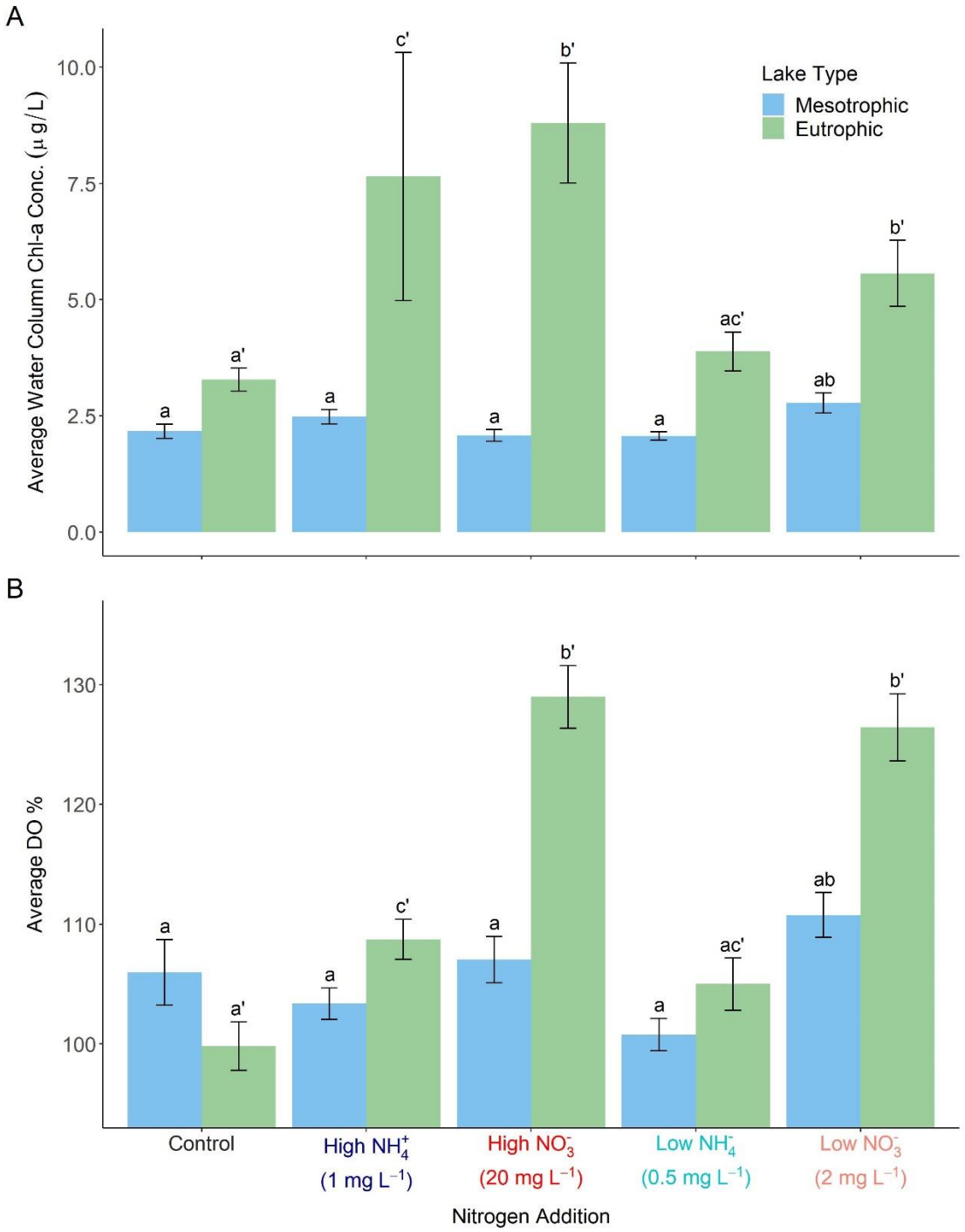

Figure 3: *Mean water column (a) chl-a concentrations and (b) percent saturation of dissolved oxygen by lake type. Error bars represent one standard error of the mean (SE; n = 42). Different letters (a-d) show significant differences among treatments (Tukey post hoc test, $p < 0.05$).*

Similar to the water column chl-a concentrations, sediment chl-a was stimulated more in the euphoric lake type compared to the mesotrophic type on both sample day 9 (contrasting high

NO_3^- eutrophic vs. mesotrophic, Tukey's post hoc test, $p<0.0001$, Figure 4a) and sample day 14 (NO_3^- eutrophic vs. mesotrophic, Tukey's post hoc test, $p=0.0033$, Figure 4b). The NO_3^- additions stimulated the most growth in the eutrophic lake (Figure 4), comparable to the water column results (Figure 3a). In contrast, N additions in the mesotrophic lake type did not significantly change sediment chl-a concentrations (contrasting mesotrophic control vs. high NO_3^-, Tukey's post hoc test, $p=0.5533$ on day 9 and $p=0.2004$ on day 14, Figure 4).

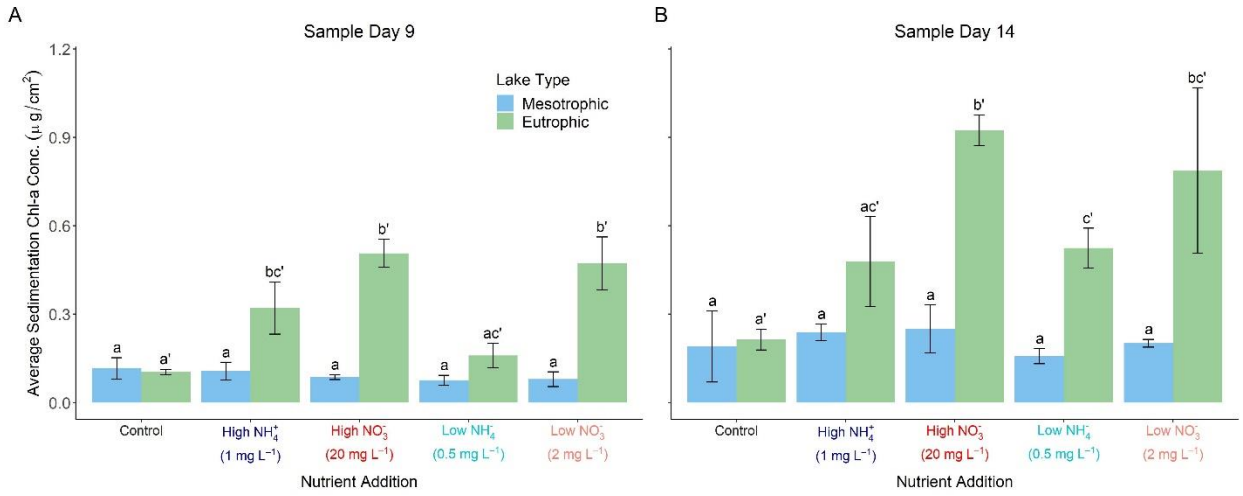

Figure 4: *Mean sediment chl-a concentrations for each lake type at the two sample time points (sample day 9 (A), and sample day (B)). Error bars represent one standard error of the mean (SE; n = 3).*

Cyanotoxin concentrations (measured as microcystin-leucine arginine (MC-LR)) were low in both the water column and sediment samples, with significantly higher toxin levels in sediment samples from two of the treatments in the eutrophic lake type on day 14 (control and low NH_4^+ treatment) (Figure 5b). Most of the water column MC-LR samples (48/60) were below detection limit (0.15 µg/L); no sediment samples were below detection. Elevated MC-LR concentrations in the mesotrophic control and low NO_3^- were driven by a single tank of the

triplicated mesocosms (Figure 5). There was also higher TSS and AFDM content in the eutrophic lake than in the mesotrophic lake.

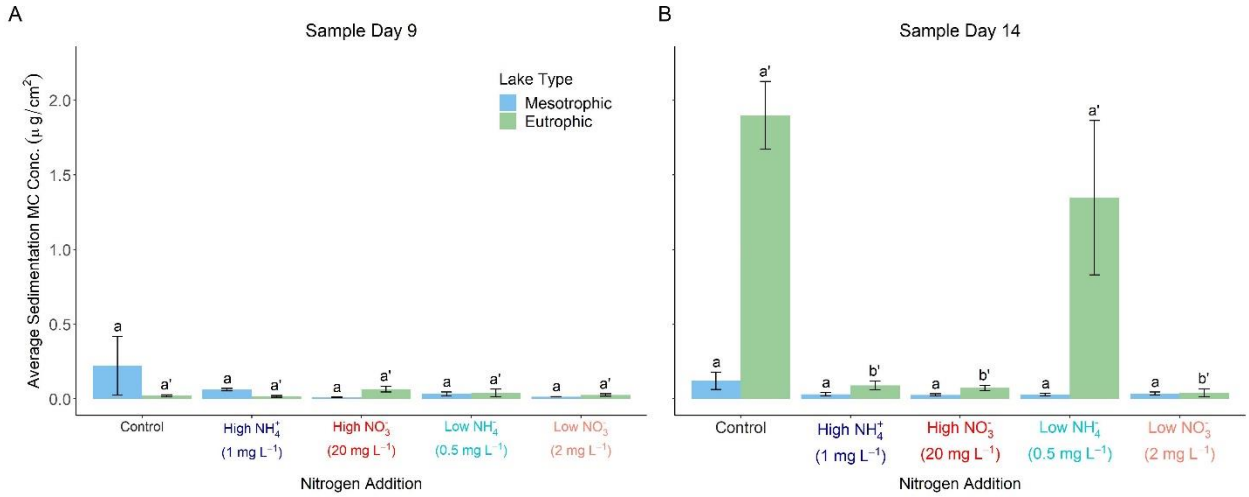

Figure 5: *Mean sediment microcystin-LR (MC-LR) concentrations for each lake type at the two sample time points (sample day 9 (A) and sample day 14 (B)). Error bars represent one standard error of the mean (SE; n = 3).*

Microbial community composition (MCC) is different in both lake types and responds to nutrient additions differently in each lake (Figure 6). In a Principal Coordinates Analysis (PCoA), the first axis accounted for 22.4% of variances, and the second axis accounted for 13.9 % of the variance. On sample day 3, the lakes MCCs are organized in distinct and separate clusters (Figure 6A). Through time, the eutrophic lake moves across axis 1 while the mesotrophic lake moves up axis 2. In the eutrophic lake, much of the shift in axis 1 is driven by the nitrate treatments. In the mesotrophic lake, shifts in axis 1 appear to be driven more by time than N additions. In the PERMANOVA model, all factors (lake, N addition, and sample day) were independently significant ($p < 0.001$; table 2). The interaction of lake and N addition, and

lake and sample day were statistically significant ($p < 0.001$; table 2). The interaction between N addition and sample day was not significant ($p = 0.057$; table 2).

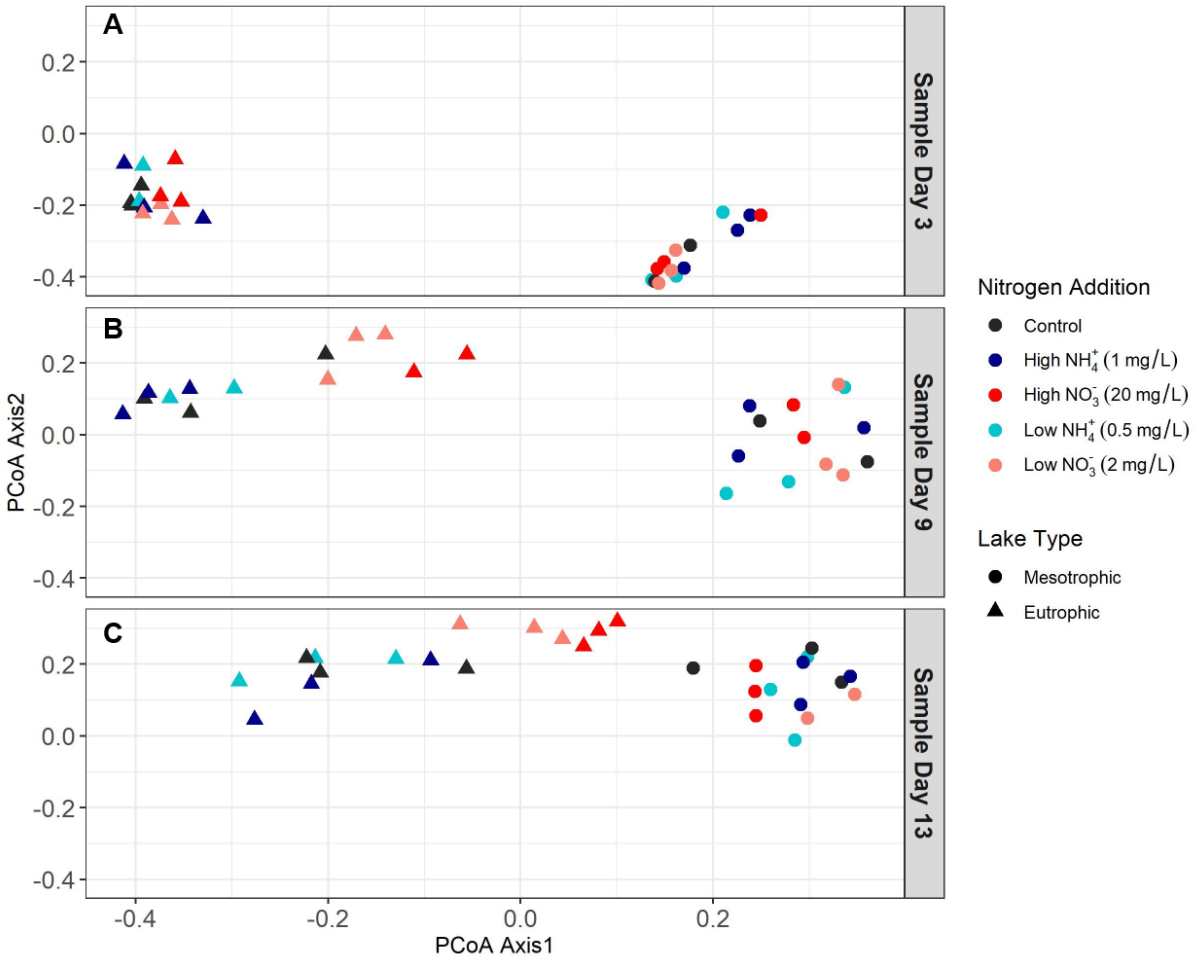

Figure 6: *Ordination of the first two axes of principal coordinate (PCoA) of Bray-Curtis distances for microbial community composition (MCC) in the water column. Data is from multiple sample days: 3, 9, and 13. Color represents the N additions and shape represents lake type. Each point represents a sample. Shorter distances between points indicate a more similar community composition rather than points further apart. Variance explained by PCoA Axis 1 = 22.4% and PCoA Axis 2 = 13.9%.*

Communities based on Bray-Curtis distances						
Source of Varaition	**Df**	**SS**	**MS**	**F**	**R^2**	**P**
Water column						
Lake type	1	5.5372	5.372	33.737	0.21433	**0.001**
N addition	4	1.7043	0.4261	2.596	0.06597	**0.001**
Sample day	1	3.4679	3.4679	21.129	0.13424	**0.001**
Lake type : N addition	4	1.2548	0.3137	1.911	0.04857	**0.001**
Lake type : Sample day	1	1.6545	1.6545	10.081	0.06404	**0.001**
N addition : Sample day	4	1.074	0.2685	1.636	0.04157	0.065
Lake type : N addition : Sample day	4	0.8015	0.2004	1.221	0.03103	0.313
Residuals	63	10.3402	0.1641		1.40024	
Total	82	25.8346			1.00000	
Sediment						
Lake type	1	2.1145	2.11454	10.4213	0.12359	**0.001**
N addition	4	1.7810	0.44524	2.1943	0.10409	**0.001**
Sample day	1	0.9491	0.94910	4.6775	0.05547	**0.001**
Lake type : N addition	4	1.5535	0.38837	1.9140	0.09080	**0.001**
Lake type : Sample day	1	0.6808	0.68084	3.3555	0.03979	**0.001**
N addition : Sample day	4	1.0177	0.25441	1.2538	0.05948	0.073
Lake type : N addition : Sample day	4	0.8965	0.22414	1.1046	0.05240	0.222
Residuals	40	8.1163	0.20291		0.47437	
Total	59	17.1094			1.00000	

Table 2: *PERMANOVA results based on Bray-Curtis distances for the water column and the sediment.*

Total relative abundance in the water column was similar in both lakes on sample day 3. N treatments did not drive MCC divergence until sample day 9 (Figure 7), which is consistent with the PCoA (Figure 6). In the mesotrophic lake, there were more sequences from the genus *Candidatus Planktophila*, *Caulobacter*, and *Sporichthyaceae* on sample day 3 (Figure 7a). In contrast, MCC in the eutrophic lake on day 3 was driven by more sequences from the genus *Cyanobium*, a genus in the Cyanobacteria family, and LD29, an unidentified eubacterium (Figure 7d). By day 9 there was a large increase of chloroplasts in the mesotrophic lake, which caused the

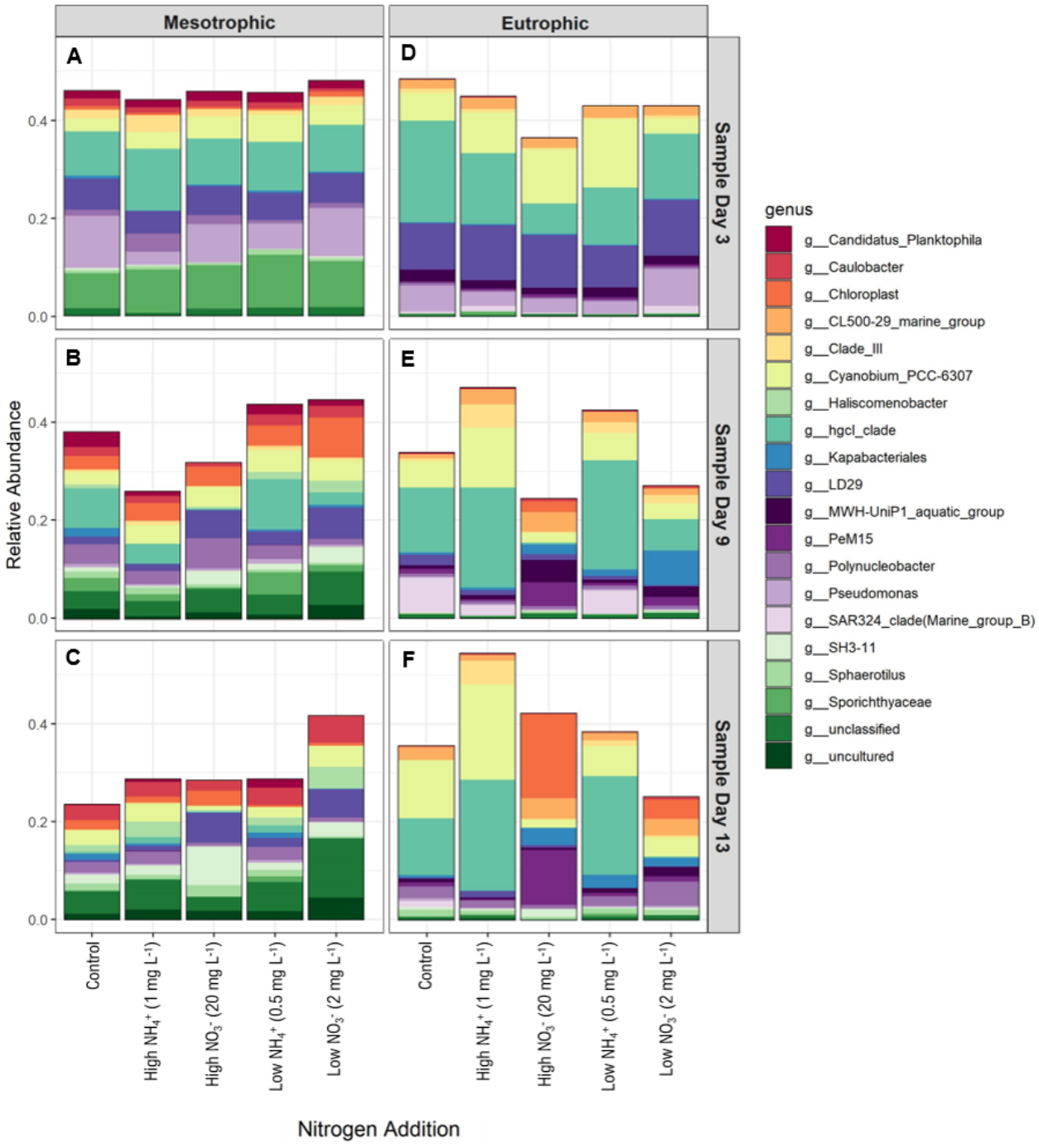

Figure 7: *Genus level microbial taxonomic composition of water column samples. The 20 most abundant genera are identified in the legend. Data compares the two different lake types (mesotrophic vs. eutrophic) and is from multiple sample days: 3, 9, and 13.*

relative abundance of the other genera to decrease (Figure 7b). The presence of high chloroplast abundance indicating a green-algae or yellow-green bloom. The eutrophic lake on sample day 9,

LD29 became distinctly less abundant, and *hgcl.clade*, a freshwater genus in the *Actinobacteria* phylum, abundance varied in response to N (Figure 7e). In the mesotrophic lake, differences in

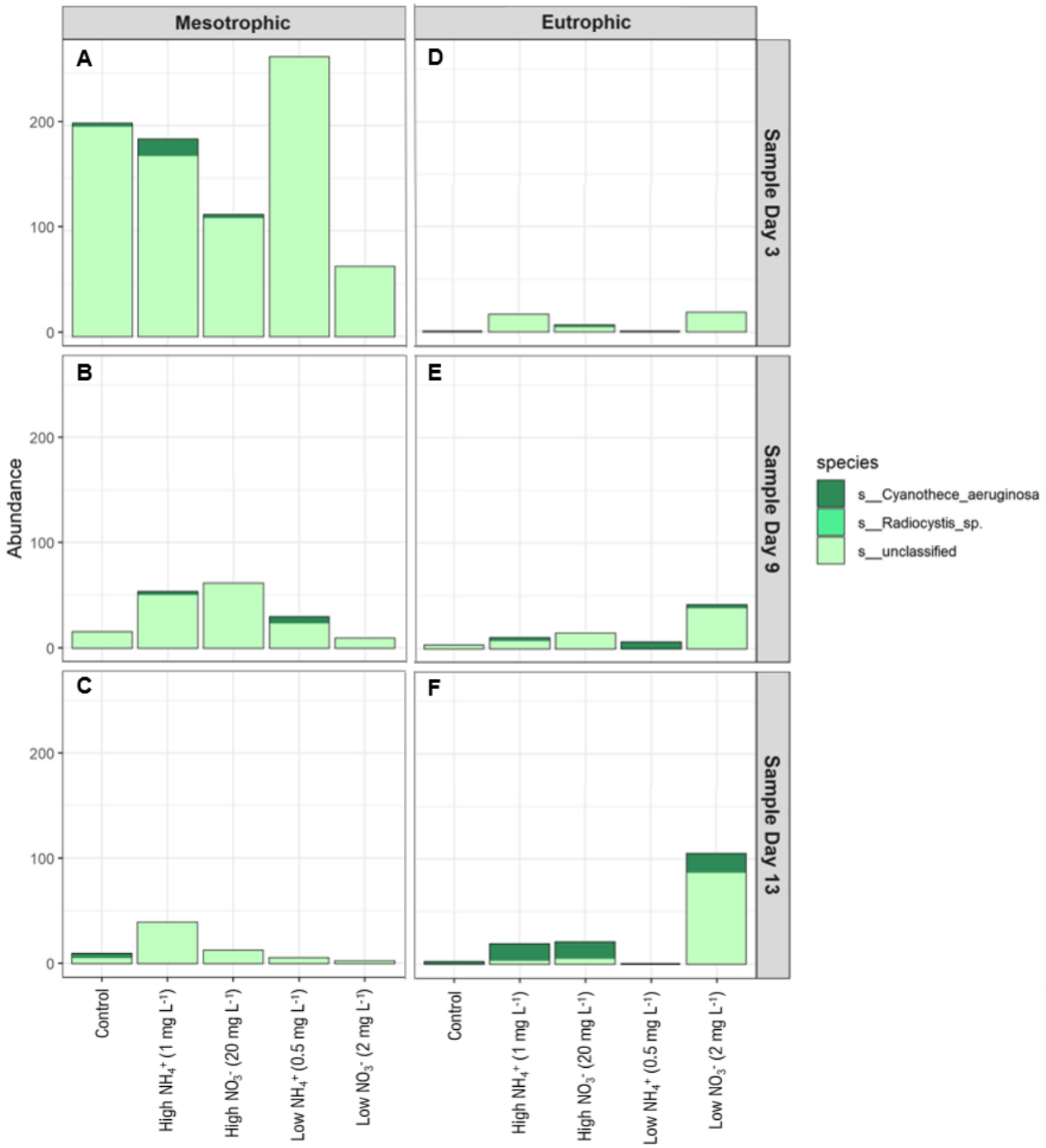

Figure 8: *Species level microbial taxonomic composition of only the Microcystis genus in water samples. Data compares the two different lake types (mesotrophic vs. eutrophic) and is from multiple sample days: 3, 9, and 13.*

MCC did not response to N or from sample day 9 to sample day 14 (Figure 7b and 7c). However, the eutrophic lake's MCC continued to change. NH_4^+ additions and the control mesocosms selected more for the *hgcl.clade* (Figure 7d-f). The genus, *Cyanobium*, continued to increase especially in the high NH_4^+ mesocosms (Figure 7d-f). In the high NO_3^- mesocosms on sample day 14, chloroplasts dramatically increased indicating a green-algae or yellow-green bloom (Figure 7f).

Although the genus, *Microcystis*, was not in the top 20 most abundant genera, *Microcystis* species were present in the mesocosms (Figure 8). On sample day 3, *Microcystis* was an order of magnitude more abundant in the mesotrophic lake (Figure 8a) compared to the eutrophic lake (Figure 8d). *Microcystis* becomes less abundant in the mesotrophic mesocosms over the course of the experiment, regardless of N treatment (Figure 8a-c). In contrast, in the eutrophic lake, *Microcystis* never becomes as abundant as it was in the day 3 mesotrophic mesocosms (Figure 8d-f). Overall, there are minor shifts in community composition within the *Microcystis* genus. However, *Cyanothece aeruginosa* becomes more abundant as the experiment progresses, particularly in the higher concentration treatments.

MCC in sediment samples shows less differentiation between the two lake types (Figure 9) than was observed in the MCC in the water column (Figure 6). The first axis accounted for 17.5% of variances, and the second axis accounted for 11.1%. On sample day 9, the two lake types are more dissimilar. In contrast, on sample day 14, the MCC in each lake are more similar and begin to merge together. In the PERMANOVA model, all factors (lake N addition, and sample day) are independently significant ($p < 0.001$). The interaction of lake and N addition, and lake and sample day were statistically significant ($p < 0.001$). The interaction between N

addition and sample day was not significant ($p = 0.058$).

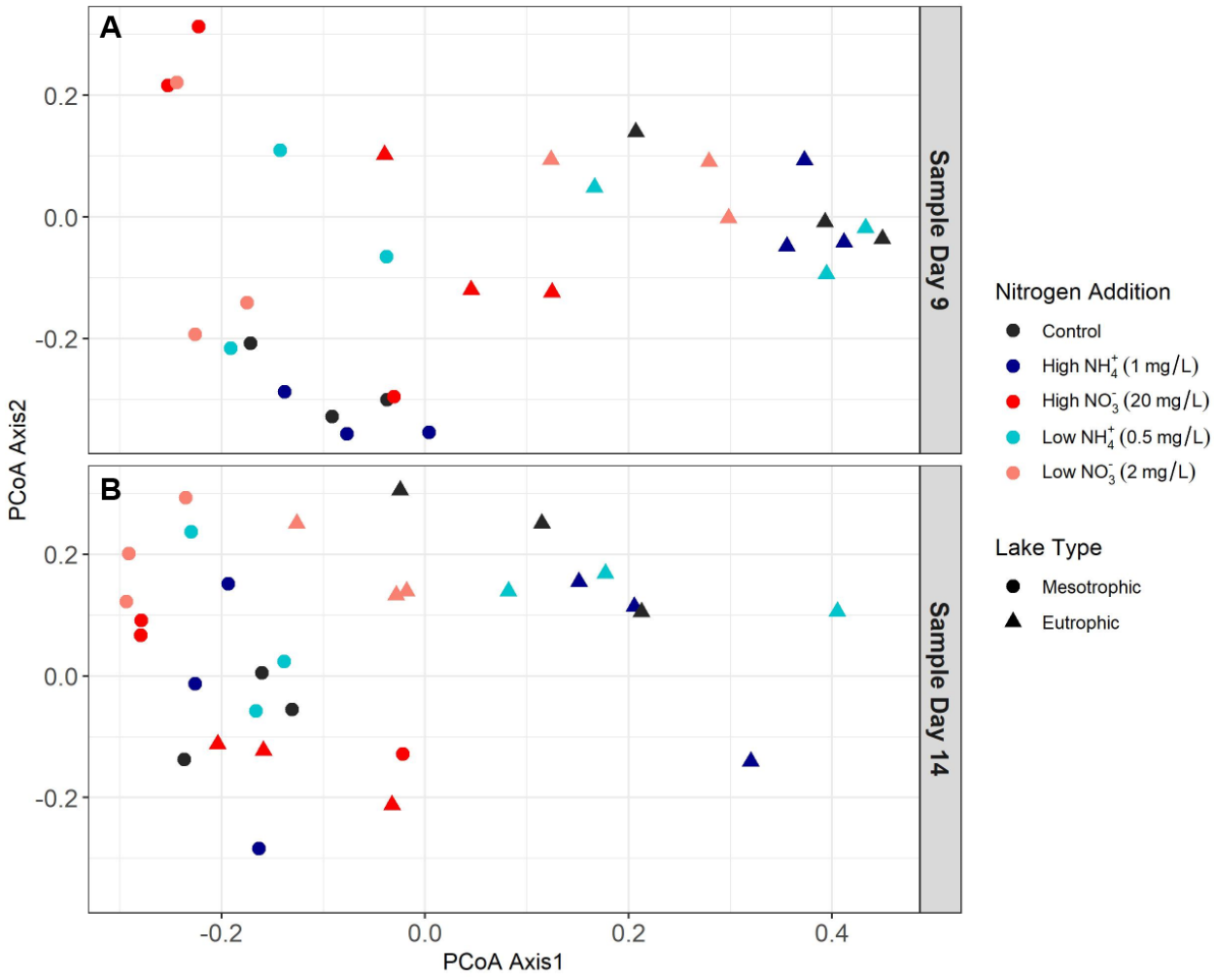

Figure 9: *Ordination of the first two axes of principal coordinate (PCoA) of Bray-Curtis distances for microbial community composition (MCC) in the sediment. Data is from two sample days: 9 (A) and 14 (B). Color represents the N additions and shape represents lake type. Each point represents a sample. Shorter distances between points indicate a more similar community composition rather than points further apart. Variance explained by PCoA Axis 1 = 17.5% and PCoA Axis 2 = 11.1%.*

There is a large difference in sediment MCC between lakes, and an individual genus increases in relative abundance with each lake through time under different N additions (Figure 10). In the mesotrophic lake, there were more sequences from the genus *Roseomonas* and Chloroplasts on sample day 9 indicating a green-algae or yellow-green bloom (Figure 10a). In

contrast, the eutrophic lake contained more sequences from the genus *Cyanobium*, a Cyanobacterium, and *Rhodobacter*, an anaerobic photosynthesizer (Figure 10c). In the mesotrophic lake, on sample day 14, *Roseomonas* becomes less abundant and uncultured bacterium become more abundant (Figure 10b). In the eutrophic lake, the high NO_3^- mesocosms has the most chloroplast abundance indicating a green-algae or yellow-green bloom, followed by

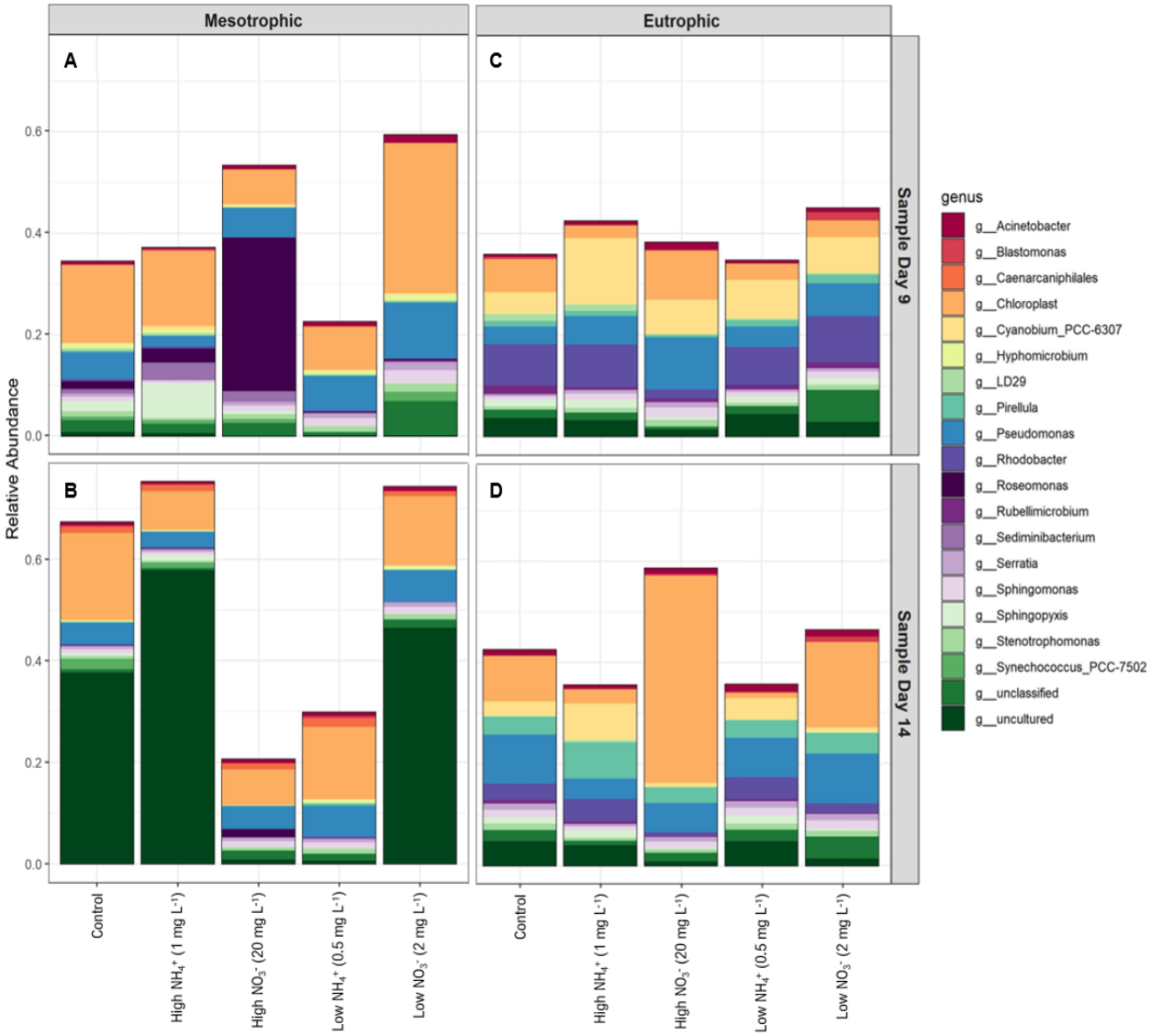

Figure 10: *Genus level microbial taxonomic composition of sediment samples. The 20 most abundant genera are identified in the legend. Data compares the two different lake types (mesotrophic vs. eutrophic) and is from two sample days: 9 and 14.*

the low NO_3^- mesocosms (Figure 10d). Overall, *Cyanobium* becomes less abundant in the sediment of the eutrophic lake (Figure 10c-d).

Microcystis was present in the sediment samples despite not being in the top 20 genera (Figure 11). However, *Microcystis* from the sediment vastly differed from the *Microcystis* from the water column in both composition and abundance (Figure 8). In the sediment samples, *Microcystis* composition is mainly compose of *Cyanothece aeruginosa*. On sample day 9, the

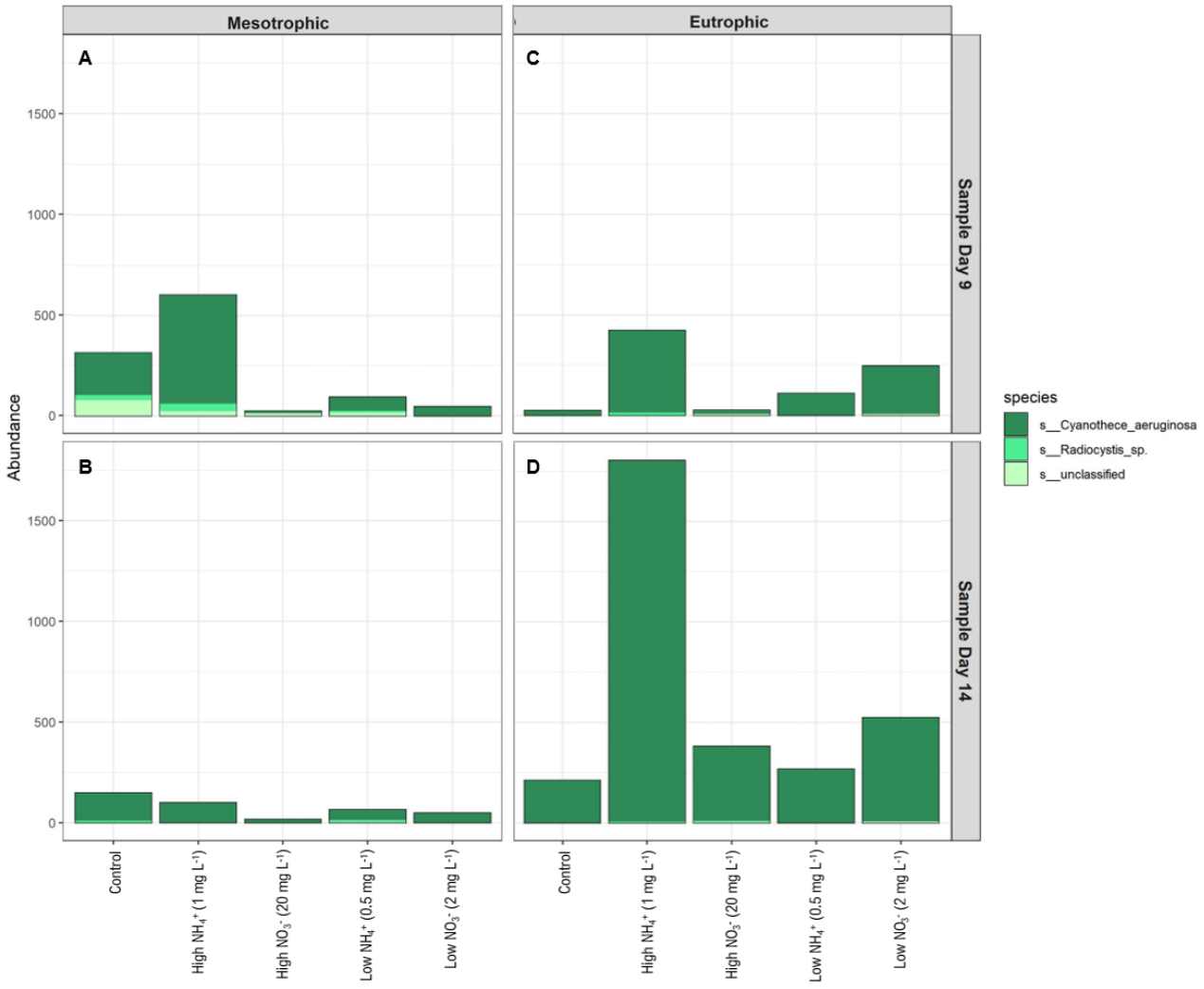

Figure 11: *Species level microbial taxonomic composition of only the Microcystis genus in water samples. Data compares the two different lake types (mesotrophic vs. eutrophic) and is from two sample days: 9 and 14*

abundance and composition in each lake are similar (Figure 11a and 11c). However, on sample day 14, the eutrophic lake had an order of magnitude higher *Microcystis*, especially in the high NH_4^+ mesocosms (Figure 11b and 11d).

Discussion

Human activities are increasing the total N lakes receive from surrounding areas, leading to eutrophication, which has been implicated in increasingly intense and frequent cyanoHABs (Paerl et al. 2001; Carmichael 2001; Merel et al. 2013; Paerl and Barnard 2020). We show that a lake's MCC, which is influenced by contrasting historical nutrient loading, can affect the response trajectory when nitrogen is increased at environmentally relevant levels. Both lakes' (mesotrophic vs. eutrophic) microbial communities changed (Figures 6 and 7), but the eutrophic lake experienced the higher overall increase in photosynthetic biomass (Figures 3 and 4). However, biomass growth (chl-a) in response to N is reliant on the form of N as well as concentration (Figures 3 and 4). We found that changes in biomass and microbial community did not result in increased toxin production (Figure 5). Below, we discuss our observations of microbial community shifts (Figure 6 and 7) as they relate to N additions for each lake type, and how this affected biomass abundance (Figure 3 and 4) and MC-LR quantities (Figure 5) in our mesocosms. We postulated that excess N conditions in a eutrophic lake would have higher potential of producing a toxic cyanoHAB. We concluded that the extant microbiome in a lake is highly influential in the formation of a cyanoHABs, even under excess N conditions.

The eutrophic lake type stimulated the most biomass growth (Figure 3 and 4) and the N additions changed the eutrophic's MCC more (Figure 6 and 9) when compared to the mesotrophic lake in both the water column and the sediment. This response is most likely due to microbiome of the eutrophic lake experiencing regular high nutrient loads; thus, it may more easily adapt to

uptake higher concentrations of N and assimilate it into biomass. The sediment samples are a reflection of what occurs in the water column, but the sediment has more biomass, and therefore, more biological activity. This is because the sediment samples are an accumulation of microbes, organic matter, and nutrients settling out of the water column. However, there is a microenvironment being created in the sediment layer at the bottom of the mesocosms. The decomposition of organic matter such as cellular phospholipid membranes, DNA/RNA, enzymes, proteins, and ATPs release excess P into the sediment. P is limited in the water column, but P could be more abundant in the sediment layer, which could also be driving shifts in the MCC to be less reflective of the water column. However, in the eutrophic lake water, *Cyanobium*, a genus of Cyanobacteria, is seen in both the water column and sediment. The NH_4^+ additions are favoring *Cyanobium*, and therefore a Cyanobacteria bloom, while NO_3^- additions are favoring chloroplasts indicating a green-algae or yellow-green bloom. These shifts are not found in the mesotrophic lake microbiome.

In the water column, N additions in the eutrophic lake stimulated biomass and shifted microbial communities, whereas, N additions in the mesotrophic lake had smaller effects on biomass (Figure 3A, Figure 4) and associated shifts the microbial communities (Figures 6 and 7). Other studies have found that N in already high nutrient lakes increases Cyanobacteria dominance and biomass (Smith 1983; Wilhelm et al. 2011). Eutrophic lakes are dominated by Cyanobacteria more than mesotrophic-oligotrophic lakes (Shen et al. 2019) a pattern which holds for both planktonic and sediment bacterial assemblages (Dai et al. 2016).

In the eutrophic lake, high NH_4^+ mesocosms shifted toward a community that favored *Cyanobium*, indicating a cyanoHAB, while high NO_3^- mesocosms shifted toward a community that favors chloroplasts, indicating a yellow or green algae bloom (Figure 7). The established

microbial community from eutrophic lakes has had time to adapt to high nutrient levels and was better able to quickly utilize the additional nutrients, which may have resulted in a dramatic increase of the copiotrophs and higher biomass production than mesotrophic communities. However, in a study using Lake Shenandoah, a highly anthropogenic impacted lake with historic heavy nutrient loads, nitrogen additions (nitrate, ammonium, and urea) did not significantly shift the bacterial community and members of the *Actinobacteria* and *Proteobacteria* phyla remained dominant across all treatments (Reynoso et al. 2019).

In the mesotrophic lake, all treatments including the control mesocosms, shift in unison and do not respond to N additions (Figure 7). Another mesocosm study using only a mesotrophic lake showed that the microbial community changed with N additions because there was a large turnover rate (Chróst et al. 2009). In other studies, it was not noted if the mesotrophic lake ever had a recorded cyanoHABs. However, in our study, the chosen mesotrophic lake has never had a recorded cyanoHAB.

Eutrophication is the growth of unabated organisms promoted by excessive nutrient (N and P) loading (Wetzel 2001; Paerl and Barnard 2020). Traditional management of excessive primary production in freshwater focused on reducing P (Schindler 1975; Levy Sharon 2017). The connection between P and Cyanobacteria are based on low N:P waters, common cyanoHAB genera (i.e. *Anabeana, Aphaizomenon, Cylindrospermopsis, Nodularia*) supply the community with N by fixing atmospheric N_2 into a more biologically available form of N, NH_3 (Schindler et al. 2008). N_2-fixing bacteria were able to balance ecosystem N deficiencies (Schindler et al. 2008; Schindler 2012; Scott et al. 2019) and diazotrophic Cyanobacteria become the dominant genera in the microbial community (Schindler 1975). However, N_2-fixing bacteria are often restricted by energetic demands and N_2-fixation is more heavily countered by denitrification, which dominates

N fluctuation resulting in a net N loss in the water-air gas exchange interface (Paerl and Otten 2016b; Paerl et al. 2018). In an ecosystem, where P is limited, N can quickly become limited due to N_2-fixation being biologically expensive. With the N additions in our study, bacteria are no long N limited, thus a competitive advantage was given to the non-N_2 fixing bacteria allowing them to grow unabated.

The stoichiometric balance between N and P has become unbalanced due to anthropogenic nutrient inputs (Conley et al. 2009; Glibert 2020) such as the growing use of synthetic N fertilizers (Glibert 2020). The more common toxigenic genera of Cyanobacteria (i.e. *Microcystis* and *Planktothrix*) are more dependent on N inputs. The strong relationship between toxic Cyanobacteria that cannot fix N and N inputs have been reported in laboratory studies (Watanabe and Oishi 1985). Also, studies have shown that increased amounts of exogenous N can shift the Cyanobacteria community from N_2-fixing to a non N_2-fixing community (Chaffin et al. 2013; Gobler et al. 2016). Despite biomass growth promoted by N additions and the presence of Cyanobacteria, our study did not see an increase of toxin production.

Cyanotoxin producing bacteria were present in the mesocosms; despite this, toxin production was low. Many studies have found inconsistent patterns in microcystin production and toxin producing cellular count (Chorus and Welker 2021). These inconsistencies can at least partially be explained by variations in methods for cell culturing, toxin measurements (i.e. ELISA, HPLC) and biomass proxy (i.e., chl-a, cell number). Also, microcystin may be underestimated as it binds to proteins and conventional methods are not adequate in detecting protein-bound MCs (Chorus and Welker 2021). The lack of microcystin could also be because the coevolved bacterial community that interacts with cyanoHAB species did not develop.

Cyanobacteria and associated bacteria have a metabolic interconnectedness and niche partitioning found by Garcia and team (Garcia et al. 2015). They uncovered that associated bacteria produce necessary nutrients, such as vitamin B12, to neighboring bacteria. This phenomenon is the *Microcystis* interactome (Garcia et al. 2015). The associated bacteria was present when *Microcystis* blooms were active in a study assessing 12 lakes spanning for continents (Cook et al. 2020). *Microcystis* have smaller genomes than other algae (Gregory et al. 2007), and are missing key metabolic functions (Steffen et al. 2012), which need to be supplemented by the metabolic functions of their associated microbial community (Morris et al. 2012; Garcia et al. 2015; Cook et al. 2020). The missing metabolic functions for the *Microcystis* species and the associated bacteria could limit the biosynthesis for cyanotoxins (Garcia et al. 2015; Cook et al. 2020). As a result, we see the presence of *Microcystis* and other Cyanobacteria, but we do not see a toxin response. Also, in the mesocosms, *Microcystis* was not within the top 20 most abundant taxa.

Although we did not see a significant increase of toxins, we saw a large increase in biomass in mesocosms where nitrogen was added, more so in the eutrophic lake. Nitrogen stimulated biomass growth and proliferated a non-toxic bloom. A non-toxic bloom still poses threat to water quality, and therefore, ecosystem health. Non-toxic blooms can deplete dissolved oxygen levels, creating hypoxia zones. These zones suffocate fish and induce mass fish kills (Kibria et al. 2019). Also, non-toxic blooms can disrupt aquatic food webs (Paerl et al. 2001). Blooms are a source of low food quality for grazers, which can echo up the food chain. Although we saw a larger increase of biomass in the eutrophic lake, if the mesotrophic lake continues to receive excess N, overtime, the mesotrophic lake will change trophic status to eutrophic and will more easily be able to proliferate a non-toxic bloom with the potential of becoming toxic. Therefore, N presents on a risk to both lake types despite the lack of a response in the mesotrophic mesocosms.

Conclusion

Elevated nitrogen concentrations do not significantly increase the amount of cyanotoxins, despite driving microbial community shifts that increased the abundance of toxic cyanoHABs. As global N inputs continue to increase, phytoplankton can grow unabated and microbial communities in freshwater ecosystems will continue to shift. In our study, the mesotrophic lake does not appear to be subject to change as strongly as the eutrophic lake. However, if the mesotrophic lake experiences longer term excess N, it would eventually be classified as eutrophic and therefore more likely to experience the same responses and shifts in the microbiome. Therefore, it is important to consider N, as well as previously studied P, when managing freshwater ecosystems and their watersheds to preserve the integrity of water quality of a mesotrophic lake and to rehabilitate a eutrophic lake.

References

Berry, M. A., T. W. Davis, R. M. Cory, and others. 2017. Cyanobacterial harmful algal blooms are a biological disturbance to Western Lake Erie bacterial communities. Environ. Microbiol. **19**: 1149–1162. doi:https://doi.org/10.1111/1462-2920.13640

Bouaïcha, N., C. O. Miles, D. G. Beach, Z. Labidi, A. Djabri, N. Y. Benayache, and T. Nguyen-Quang. 2019. Structural Diversity, Characterization and Toxicology of Microcystins.doi:10.20944/preprints201910.0034.v1

Brooks, B. W., J. M. Lazorchak, M. D. A. Howard, and others. 2016. Are harmful algal blooms becoming the greatest inland water quality threat to public health and aquatic ecosystems? Environ. Toxicol. Chem. **35**: 6–13. doi:10.1002/etc.3220

Callahan, B. J., P. J. McMurdie, M. J. Rosen, A. W. Han, A. J. A. Johnson, and S. P. Holmes. 2016. DADA2: High resolution sample inference from Illumina amplicon data. Nat. Methods **13**: 581–583. doi:10.1038/nmeth.3869

Caporaso, J. G., C. L. Lauber, W. A. Walters, and others. 2012. Ultra-high-throughput microbial community analysis on the Illumina HiSeq and MiSeq platforms. ISME J. **6**: 1621–1624. doi:10.1038/ismej.2012.8

Carmichael, W. W. 2001. Health Effects of Toxin-Producing Cyanobacteria: "The CyanoHABs." Hum. Ecol. Risk Assess. Int. J. **7**: 1393–1407. doi:10.1080/20018091095087

Carmichael, W. W., S. M. Azevedo, J. S. An, and others. 2001. Human fatalities from cyanobacteria: chemical and biological evidence for cyanotoxins. Environ. Health Perspect. **109**: 663–668.

Carmichael, W. W., and G. L. Boyer. 2016. Health impacts from cyanobacteria harmful algae blooms: Implications for the North American Great Lakes. Harmful Algae **54**: 194–212. doi:10.1016/j.hal.2016.02.002

Carpenter, S. R., N. F. Caraco, D. L. Correll, R. W. Howarth, A. N. Sharpley, and V. H. Smith. 1998. Nonpoint Pollution of Surface Waters with Phosphorus and Nitrogen. Ecol. Appl. **8**: 559–568. doi:10.1890/1051-0761(1998)008[0559:NPOSWW]2.0.CO;2

Chaffin, J. D., T. B. Bridgeman, and D. L. Bade. 2013. Nitrogen Constrains the Growth of Late Summer Cyanobacterial Blooms in Lake Erie. Adv. Microbiol. **3**: 720–726. doi:10.4236/aim.2013.36A003

Chaffin, J. D., T. W. Davis, D. J. Smith, M. M. Baer, and G. J. Dick. 2018. Interactions between nitrogen form, loading rate, and light intensity on Microcystis and Planktothrix growth and microcystin production. Harmful Algae **73**: 84–97. doi:10.1016/j.hal.2018.02.001

Chapin, B., F..DeNoyelles, D.W. Graham, and V.H. Smith. 2004. A deep maximum of green sulphur bacteria (‘Chlorochromatium aggregatum’) in a strongly stratified reservoir. Freshwater Biology. doi:10.1111/j.1365-2427.2004.01270.x

Chorus, I., and J. Bartram, eds. 2021. Toxic cyanobacteria in water: a guide to their public health consequences, monitoring, and management, 2nd ed. E & FN Spon.

Chorus, I., I. R. Falconer, H. J. Salas, and J. Bartram. 2000. Health risks caused by freshwater cyanobacteria in recreational waters. J. Toxicol. Environ. Health B Crit. Rev. **3**: 323–347. doi:10.1080/109374000436364

Chorus, I., and M. Welker. 2021. Cyanobacterial toxins, p. 21–159. *In* Toxic Cyanobacteria in Water. CRC Press.

Chróst, R. J., T. Adamczewski, K. Kalinowska, and A. Skowrońska. 2009. Inorganic phosphorus and nitrogen modify composition and diversity of microbial communities in water of mesotrophic lake. Pol. J. Microbiol. **58**: 77–90.

Conley, D. J., H. W. Paerl, R. W. Howarth, D. F. Boesch, S. P. Seitzinger, K. E. Havens, C. Lancelot, and G. E. Likens. 2009. Ecology. Controlling eutrophication: nitrogen and phosphorus. Science **323**: 1014–1015. doi:10.1126/science.1167755

Cook, K. V., C. Li, H. Cai, and others. 2020. The global Microcystis interactome. Limnol. Oceanogr. **65**: S194–S207. doi:10.1002/lno.11361

Dai, Y., Y. Yang, Z. Wu, Q. Feng, S. Xie, and Y. Liu. 2016. Spatiotemporal variation of planktonic and sediment bacterial assemblages in two plateau freshwater lakes at different trophic status. Appl. Microbiol. Biotechnol. **100**: 4161–4175. doi:10.1007/s00253-015-7253-2

DeAngelis, K. M., W. L. Silver, A. W. Thompson, and M. K. Firestone. 2010. Microbial communities acclimate to recurring changes in soil redox potential status. Environ. Microbiol. **12**: 3137–3149. doi:10.1111/j.1462-2920.2010.02286.x

Dodds, W. K., W. W. Bouska, J. L. Eitzmann, T. J. Pilger, K. L. Pitts, A. J. Riley, J. T. Schloesser, and D. J. Thornbrugh. 2009. Eutrophication of U.S. freshwaters: analysis of potential economic damages. Environ. Sci. Technol. **43**: 12–19. doi:10.1021/es801217q

Donald, D. B., M. J. Bogard, K. Finlay, and P. R. Leavitt. 2011. Comparative effects of urea, ammonium, and nitrate on phytoplankton abundance, community composition, and toxicity in hypereutrophic freshwaters. Limnol. Oceanogr. **56**: 2161–2175. doi:https://doi.org/10.4319/lo.2011.56.6.2161

Finlay, K., A. Patoine, D. B. Donald, M. J. Bogard, and P. R. Leavitt. 2010. Experimental evidence that pollution with urea can degrade water quality in phosphorus-rich lakes of the Northern Great Plains. Limnol. Oceanogr. **55**: 1213–1230. doi:10.4319/lo.2010.55.3.1213

Flores, E., J. E. Frías, L. M. Rubio, and A. Herrero. 2005. Photosynthetic nitrate assimilation in cyanobacteria. Photosynth. Res. **83**: 117–133. doi:10.1007/s11120-004-5830-9

Garcia, S. L., M. Buck, K. D. McMahon, H.-P. Grossart, A. Eiler, and F. Warnecke. 2015. Auxotrophy and intrapopulation complementary in the “interactome” of a cultivated freshwater model community. Mol. Ecol. **24**: 4449–4459. doi:10.1111/mec.13319

Glibert, P. M. 2020. Harmful algae at the complex nexus of eutrophication and climate change. Harmful Algae **91**: 101583. doi:10.1016/j.hal.2019.03.001

Gobler, C. J., J. M. Burkholder, T. W. Davis, M. J. Harke, T. Johengen, C. A. Stow, and D. B. Van de Waal. 2016. The dual role of nitrogen supply in controlling the growth and toxicity of cyanobacterial blooms. Harmful Algae **54**: 87–97. doi:10.1016/j.hal.2016.01.010

Gopal, S., Y. Yang, B. Bai, and A. Niculescu-Mizil. 2012. Bayesian models for large-scale hierarchical classification. *Proceedings of the 25th International Conference on Neural Information Processing Systems - Volume 2*. Curran Associates Inc. 2411–2419.

Gregory, T. R., J. A. Nicol, H. Tamm, and others. 2007. Eukaryotic genome size databases. Nucleic Acids Res. **35**: D332-338. doi:10.1093/nar/gkl828

Herrero, A., A. M. Muro-Pastor, and E. Flores. 2001. Nitrogen control in cyanobacteria. J. Bacteriol. **183**: 411–425. doi:10.1128/JB.183.2.411-425.2001

Hutchinson, G. E. 1972. Nutrients and eutrophication. Limnol. Oceanogr. **17**: 965–968. doi:10.4319/lo.1972.17.6.0965

Imanishi, S., and K. Harada. 2004. Proteomics approach on microcystin binding proteins in mouse liver for investigation of microcystin toxicity. Toxicon Off. J. Int. Soc. Toxinology **43**: 651–659. doi:10.1016/j.toxicon.2004.02.026

Kérouel, R., and A. Aminot. 1997. Fluorometric determination of ammonia in sea and estuarine waters by direct segmented flow analysis. Mar. Chem. **57**: 265–275. doi:10.1016/S0304-4203(97)00040-6

Kibria, G., A. K. Haroon, D. Nugegoda, and Md. M. Hossain. 2019. Nutrient Pollution Causing Algal Blooms, Hypoxia (Dead Zones) Across the Globe Impacting Ecosystems, Biodiversity, Public Health & Livelihoods,.

Levy Sharon. 2017. Microcystis Rising: Why Phosphorus Reduction Isn't Enough to Stop CyanoHABs. Environ. Health Perspect. **125**: A34–A39. doi:10.1289/ehp.125-A34

Linville, R., N. Butler, and B. Washburn. 2009. MICROCYSTINS: A Brief Overview of their Toxicity and Effects, with Special Reference to fish, Wildlife and Livestock. 21.

Massey, I. Y., M. A. osman, and F. Yang. 2020. An overview on cyanobacterial blooms and toxins production: their occurrence and influencing factors. Toxin Rev. **0**: 1–21. doi:10.1080/15569543.2020.1843060

McMurdie, P. J., and S. Holmes. 2013. phyloseq: an R package for reproducible interactive analysis and graphics of microbiome census data. PloS One **8**: e61217. doi:10.1371/journal.pone.0061217

Merel, S., D. Walker, R. Chicana, S. Snyder, E. Baurès, and O. Thomas. 2013. State of knowledge and concerns on cyanobacterial blooms and cyanotoxins. Environ. Int. **59**: 303–327. doi:10.1016/j.envint.2013.06.013

Metcalf, J. S., and N. R. Souza. 2019. Chapter 6 - Cyanobacteria and Their Toxins, p. 125–148. *In* S. Ahuja [ed.], Separation Science and Technology. Academic Press.

Monchamp, M.-E., F. R. Pick, B. E. Beisner, and R. Maranger. 2014. Nitrogen Forms Influence Microcystin Concentration and Composition via Changes in Cyanobacterial Community Structure B. Neilan [ed.]. PLoS ONE **9**: e85573. doi:10.1371/journal.pone.0085573

Morris, J. J., R. E. Lenski, and E. R. Zinser. 2012. The Black Queen Hypothesis: evolution of dependencies through adaptive gene loss. mBio **3**: e00036-12. doi:10.1128/mBio.00036-12

Oksanen, J., F. G. Blanchet, M. Friendly, and others. 2020. vegan: Community Ecology Package,.

Paerl, H. W., and M. A. Barnard. 2020. Mitigating the global expansion of harmful cyanobacterial blooms: Moving targets in a human- and climatically-altered world. Harmful Algae **96**: 101845. doi:10.1016/j.hal.2020.101845

Paerl, H. W., R. S. Fulton, P. H. Moisander, and J. Dyble. 2001. Harmful Freshwater Algal Blooms, With an Emphasis on Cyanobacteria. Sci. World J. **1**: 76–113. doi:10.1100/tsw.2001.16

Paerl, H. W., K. E. Havens, H. Xu, and others. 2020. Mitigating eutrophication and toxic cyanobacterial blooms in large lakes: The evolution of a dual nutrient (N and P) reduction paradigm. Hydrobiologia **847**: 4359–4375. doi:10.1007/s10750-019-04087-y

Paerl, H. W., and T. G. Otten. 2013. Harmful cyanobacterial blooms: causes, consequences, and controls. Microb. Ecol. **65**: 995–1010. doi:10.1007/s00248-012-0159-y

Paerl, H. W., and T. G. Otten. 2016a. Duelling 'CyanoHABs': unravelling the environmental drivers controlling dominance and succession among diazotrophic and non-N2-fixing harmful cyanobacteria. Environ. Microbiol. **18**: 316–324. doi:https://doi.org/10.1111/1462-2920.13035

Paerl, H. W., T. G. Otten, and R. Kudela. 2018. Mitigating the Expansion of Harmful Algal Blooms Across the Freshwater-to-Marine Continuum. Environ. Sci. Technol. **52**: 5519–5529. doi:10.1021/acs.est.7b05950

Qin, B., J. Zhou, J. J. Elser, W. S. Gardner, J. Deng, and J. D. Brookes. 2020. Water Depth Underpins the Relative Roles and Fates of Nitrogen and Phosphorus in Lakes. Environ. Sci. Technol. **54**: 3191–3198. doi:10.1021/acs.est.9b05858

Quast, C., E. Pruesse, P. Yilmaz, J. Gerken, T. Schweer, P. Yarza, J. Peplies, and F. O. Glöckner. 2013. The SILVA ribosomal RNA gene database project: improved data processing and web-based tools. Nucleic Acids Res. **41**: D590–D596. doi:10.1093/nar/gks1219

Reynoso, G., M. R. Smith, C. P. Holmes II, and others. 2019. Bacterial community structure and response to nitrogen amendments in Lake Shenandoah (VA, USA). Water Sci. Technol. **80**: 675–684. doi:10.2166/wst.2019.311

Schindler, D. W. 1975. Whole-lake eutrophication experiments with phosphorus, nitrogen and carbon. SIL Proc. 1922-2010 **19**: 3221–3231. doi:10.1080/03680770.1974.11896436

Schindler, D. W. 2012. The dilemma of controlling cultural eutrophication of lakes. Proc. R. Soc. B Biol. Sci. **279**: 4322–4333. doi:10.1098/rspb.2012.1032

Schindler, D. W., R. E. Hecky, D. L. Findlay, and others. 2008. Eutrophication of lakes cannot be controlled by reducing nitrogen input: results of a 37-year whole-ecosystem experiment. Proc. Natl. Acad. Sci. U. S. A. **105**: 11254–11258. doi:10.1073/pnas.0805108105

Scott, J. T., M. J. McCarthy, and H. W. Paerl. 2019. Nitrogen transformations differentially affect nutrient-limited primary production in lakes of varying trophic state. Limnol. Oceanogr. Lett. **4**: 96–104. doi:10.1002/lol2.10109

Shen, M., Q. Li, M. Ren, Y. Lin, J. Wang, L. Chen, T. Li, and J. Zhao. 2019. Trophic Status Is Associated With Community Structure and Metabolic Potential of Planktonic Microbiota in Plateau Lakes. Front. Microbiol. **10**: 2560. doi:10.3389/fmicb.2019.02560

Sivonen, K., and G. Jones. 1999. Cyanobacterial toxins. Toxic Cyanobacteria Water Guide Public Health Significance Monit. Manag. Chorus J Bertram Eds P 41-111 World Health Organ. ISBN 0-419-23930-8 E FN Spon Lond. UK.

Smith, V. H. 1983b. Low Nitrogen to Phosphorus Ratios Favor Dominance by Blue-Green Algae in Lake Phytoplankton. Science **221**: 669–671. doi:10.1126/science.221.4611.669

Smith, V. H. 1986. Light and Nutrient Effects on the Relative Biomass of Blue-Green Algae in Lake Phytoplankton. Can. J. Fish. Aquat. Sci. **43**: 148–153. doi:10.1139/f86-016

Smith, V. H. 2003. Eutrophication of freshwater and coastal marine ecosystems a global problem. Environ. Sci. Pollut. Res. **10**: 126–139. doi:10.1065/espr2002.12.142

Spoof, L., and A. Catherine. 2016. Appendix 3: Tables of Microcystins and Nodularins, p. 526–537. *In* Handbook of Cyanobacterial Monitoring and Cyanotoxin Analysis. John Wiley & Sons, Ltd.

Steffen, M. M., Z. Li, T. C. Effler, L. J. Hauser, G. L. Boyer, and S. W. Wilhelm. 2012. Comparative metagenomics of toxic freshwater cyanobacteria bloom communities on two continents. PloS One **7**: e44002. doi:10.1371/journal.pone.0044002

Svirčev, Z., D. Drobac, N. Tokodi, B. Mijović, G. A. Codd, and J. Meriluoto. 2017. Toxicology of microcystins with reference to cases of human intoxications and epidemiological investigations of exposures to cyanobacteria and cyanotoxins. Arch. Toxicol. **91**: 621–650. doi:10.1007/s00204-016-1921-6

Testai, E., S. Scardala, S. Vichi, F. M. Buratti, and E. Funari. 2016. Risk to human health associated with the environmental occurrence of cyanobacterial neurotoxic alkaloids anatoxins and saxitoxins. Crit. Rev. Toxicol. **46**: 385–419. doi:10.3109/10408444.2015.1137865

Vasconcelos, V. M., K. Sivonen, W. R. Evans, W. W. Carmichael, and M. Namikoshi. 1996. Hepatotoxic microcystin diversity in cyanobacterial blooms collected in portuguese freshwaters. Water Res. **30**: 2377–2384. doi:10.1016/0043-1354(96)00152-2

Wagner, N. D., E. Quach, S. Buscho, and others. 2021. Nitrogen form, concentration, and micronutrient availability affect microcystin production in cyanobacterial blooms. Harmful Algae **103**: 102002. doi:10.1016/j.hal.2021.102002

Watanabe, M. F., and S. Oishi. 1985. Effects of environmental factors on toxicity of a cyanobacterium (Microcystis aeruginosa) under culture conditions. Appl. Environ. Microbiol. **49**: 1342–1344. doi:10.1128/aem.49.5.1342-1344.1985

Wetzel, R. G. 2001. Limnology: lake and river ecosystems, 3rd ed. San Diego : Academic Press, [2001].

Wilhelm, S. W., G. S. Bullerjahn, and R. M. L. McKay. 2020. The Complicated and Confusing Ecology of Microcystis Blooms. mBio **11**: e00529-20. doi:10.1128/mBio.00529-20

Wilhelm, S. W., S. E. Farnsley, G. R. LeCleir, and others. 2011. The relationships between nutrients, cyanobacterial toxins and the microbial community in Taihu (Lake Tai), China. Harmful Algae **10**: 207–215. doi:10.1016/j.hal.2010.10.001

Zanchett, G., and E. C. Oliveira-Filho. 2013. Cyanobacteria and Cyanotoxins: From Impacts on Aquatic Ecosystems and Human Health to Anticarcinogenic Effects. Toxins **5**: 1896–1917. doi:10.3390/toxins5101896

Zurawell, R. W., H. Chen, J. M. Burke, and E. E. Prepas. 2005. Hepatotoxic Cyanobacteria: A Review of the Biological Importance of Microcystins in Freshwater Environments. J. Toxicol. Environ. Health Part B **8**: 1–37. doi:10.1080/10937400590889412

Supplemental Information

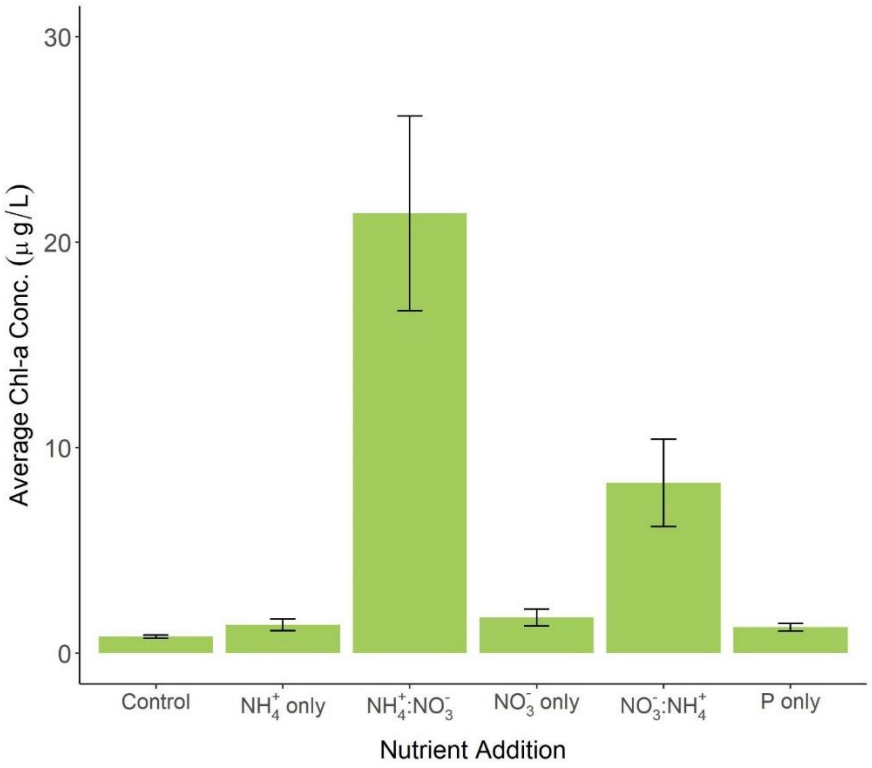

Supplemental Information Figure A: *Mean water column chl-a concentrations from pilot study (Spring 2019). Treatments include a control (no nutrient addition), NH_4^+ only, NH_4^+:NO_3^-, NO_3^- only, NO_3^-:NH_4^+, P only. Error bars represent one standard error of the mean (SE; n=3).*

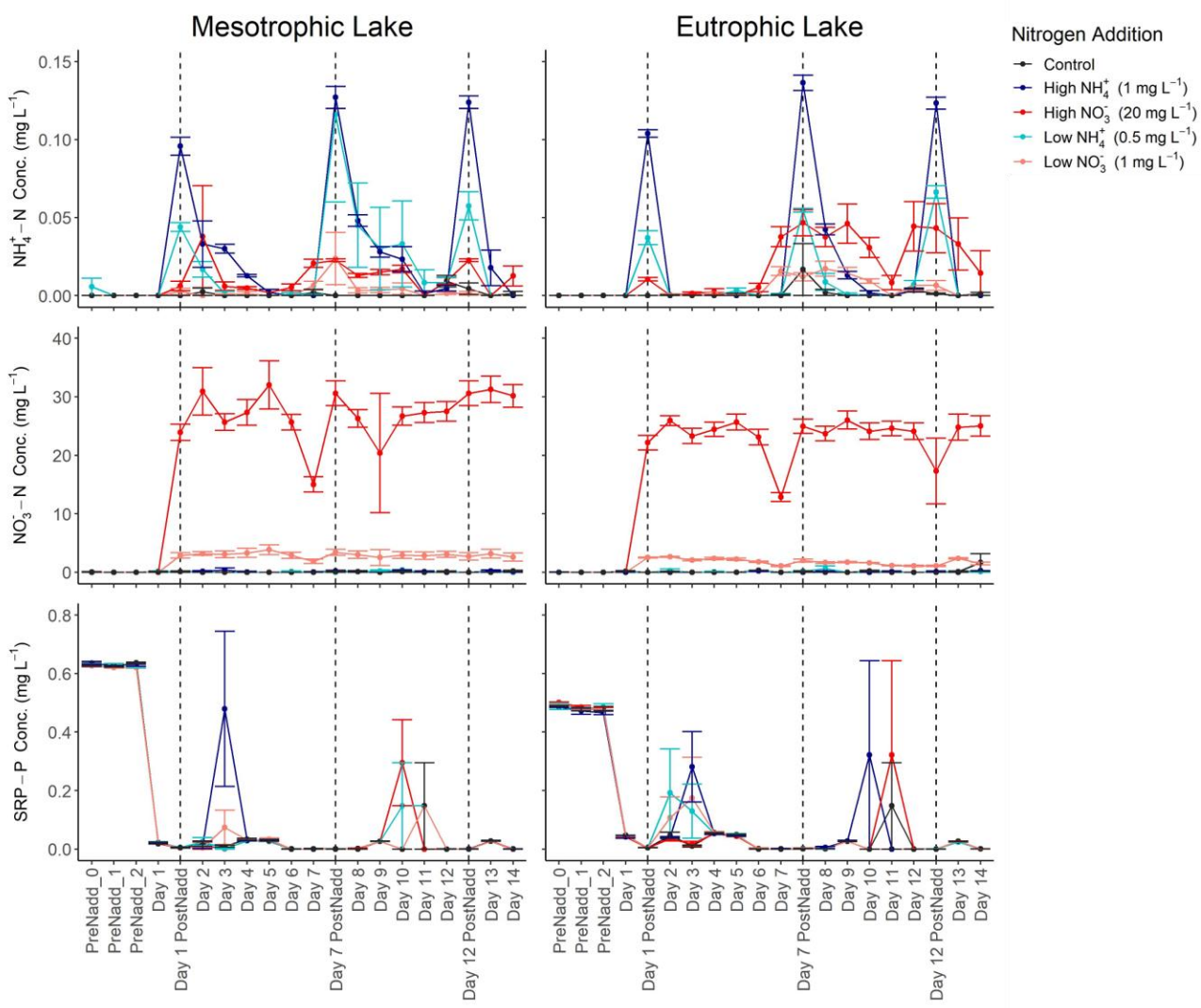

Supplemental Information Figure B: *Mean water column NH_4^+-N (a and d), NO_3^--N (b and e), SRP-P (c and f) concentrations in Error bars represent one standard error of the mean (SE; n=3).*

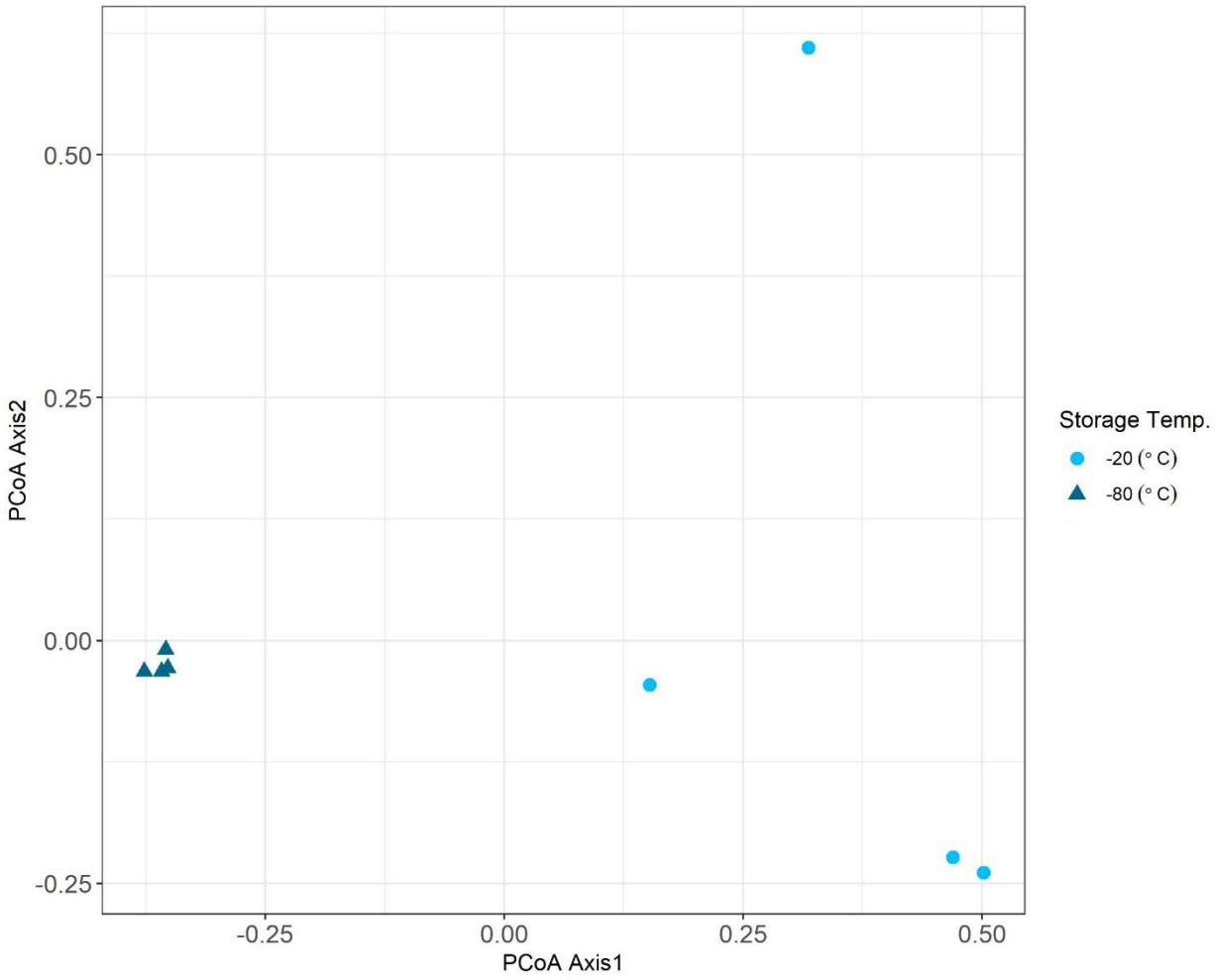

Supplemental Information Figure C: *Ordination of the first two axes of principal coordinate (PCoA) of Bray-Curtis distances for microbial community composition (MCC) comparing sample storage at two different temperatures (-20°C vs. -80°C). Color/shape represents storage temperature. Each point represents a sample. Shorter distances between points indicate a more similar community composition rather than points further apart. Variance explained by PCoA Axis 1 = 51.3% and PCoA Axis 2 = 22.3%.*

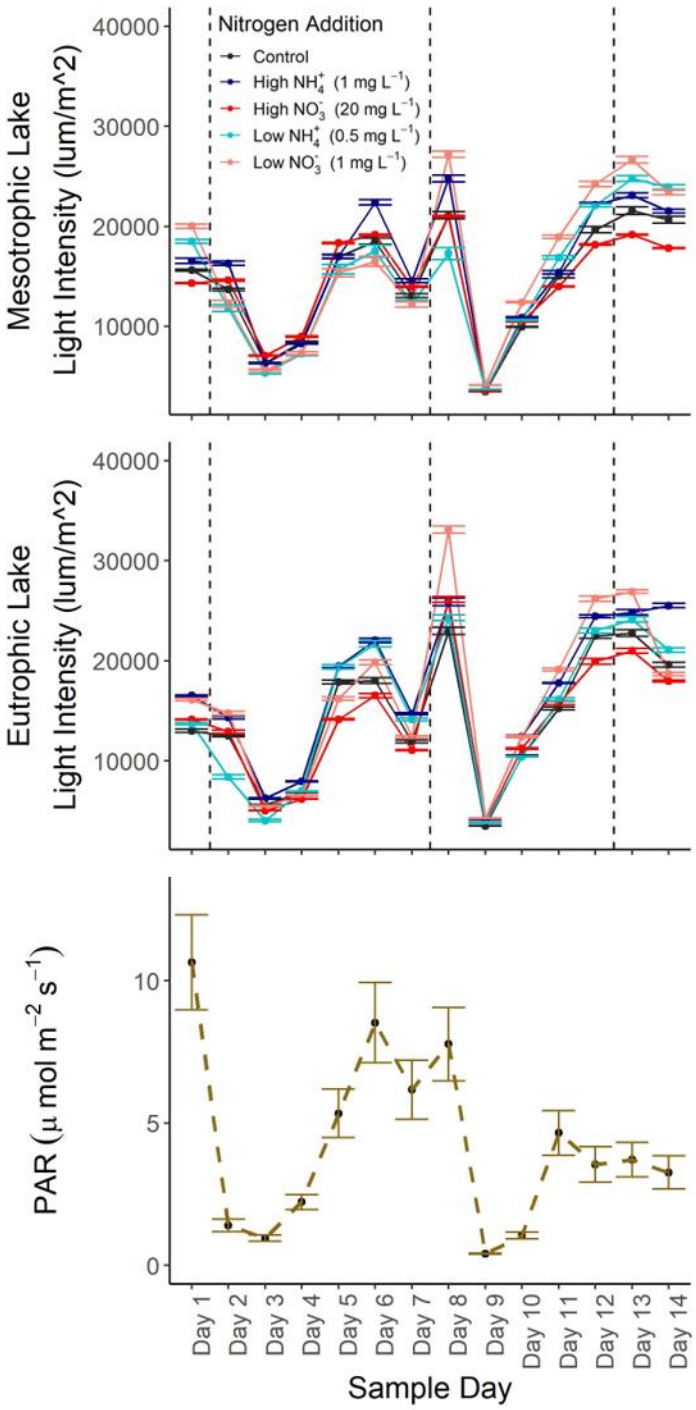

Supplemental Information Figure D: *A comparison of light intensity trends from inside each mesocosm and NEON's PAR sensor outside of the greenhouse. Error bars represent one standard error of the mean (SE).*

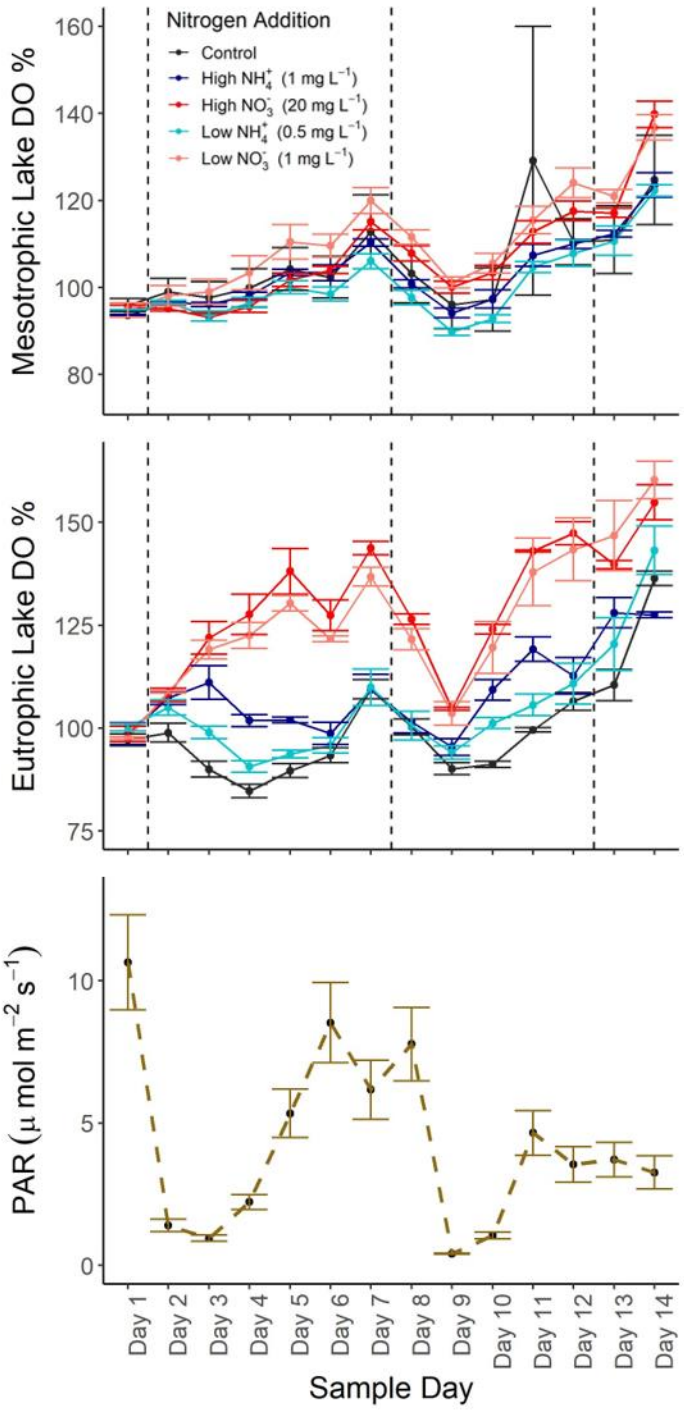

Supplemental Information Figure E: *Light intensity is autocorrelated with DO.*